THE WARNING TIME FOR CLOUD-TO-GROUND LIGHTNING IN ISOLATED, ORDINARY THUNDERSTORMS OVER HOUSTON, TEXAS

A Thesis

by

NATHAN CHASE CLEMENTS

Submitted to the Office of Graduate Studies of
Texas A&M University
in partial fulfillment of the requirements for the degree of

MASTER OF SCIENCE

December 2007

Major Subject: Atmospheric Sciences

THE WARNING TIME FOR CLOUD-TO-GROUND LIGHTNING IN ISOLATED, ORDINARY THUNDERSTORMS OVER HOUSTON, TEXAS

A Thesis

by

NATHAN CHASE CLEMENTS

Submitted to the Office of Graduate Studies of
Texas A&M University
in partial fulfillment of the requirements for the degree of

MASTER OF SCIENCE

Approved by:

Chair of Committee, Richard E. Orville
Committee Members, Larry Carey
Andrew Klein
Head of Department, Richard E. Orville

December 2007

Major Subject: Atmospheric Sciences

ABSTRACT

The Warning Time for Cloud-to-Ground Lightning in Isolated, Ordinary Thunderstorms Over Houston, Texas. (December 2007)

Nathan Chase Clements, B.S., Texas A&M University

Chair of Advisory Committee: Dr. Richard E. Orville

Lightning detection over Houston, Texas is possible with the Lightning Detection and Ranging (LDAR-II) network and the National Lightning Detection Network (NLDN). A comparison of the two datasets in conjunction with 37 isolated, ordinary thunderstorms reveals a time separation of 3.1 minutes between the first detected Very High Frequency (VHF) source (i.e. first intracloud discharge) and the first cloud-to-ground (CG) lightning flash. This CG warning time is increased to 16.1 minutes when using the radar-defined criterion of when the 30-dBZ contour first reaches the -10°C isotherm level.

Several attempts were made to establish a similar characteristic that could be used to forewarn the occurrence of the final CG in this storm type. Based on the average radar characteristics during the last CG flash in each thunderstorm case, CG activity comes to an end when the 45-dBZ echo falls below the -10°C isotherm.

Detection efficiencies that remain slightly less than perfect for each network may have allowed for some error when analyzing VHF sources and ground flashes for each

convective case. Exhibiting this possible error, four cases actually recorded a greater number of CG flashes than intracloud flashes, which is contrary to typical lightning characteristics.

Future studies hope to increase the number of thunderstorm cases to analyze as the LDAR network continues to observe more lightning events. Also, similar approaches could be implemented in differing geographic regions of the country to observe if these lightning characteristics vary depending on latitude, longitude, or climate.

ACKNOWLEDGEMENTS

I would like to give a generous thank you to my committee chair, Dr. Richard Orville, and my committee members, Dr. Larry Carey and Dr. Andrew Klein. I would also like to thank Dr. Ping Yang for substituting in place of Dr. Carey, who could not be here for my defense. Without their advice, continuous support, and direction, this work would not have been possible.

I would also like to thank my peers for their help in classes, research, and for their source of motivation and encouragement throughout the entirety of this project. I would like to individually acknowledge Chas Hodapp, Joe Jurecka, Shane Motley, Brandon Ely, and Chris McKinney for their patience with my many questions and as a source of entertainment during the difficult times.

I owe my deepest debt of gratitude to my family. They have provided me with continuous support and encouragement throughout my entire academic career. I would not be where I am now without them. Thank you everyone for helping make this project possible.

TABLE OF CONTENTS

Page

Page

LIST OF FIGURES

FIGURE Page

LIST OF TABLES

1. INTRODUCTION

1.1 Lightning and Its Importance

Lightning is a natural but destructive phenomenon that affects various locations on the earth's surface every year. Uman (1986) defines lightning as a self-propagating atmospheric electrical discharge that results from the accumulation of positive and negative space charge, typically occurring within convective clouds. This electrical discharge can occur in two basic ways: cloud flashes and ground flashes (MacGorman and Rust 1998, p. 83). The latter affects human activity, property and life. Curran et al. (2000) find that lightning is ranked second behind flash and river flooding as causing the most deaths from any weather-related event in the United States. From 1959 to 1994, there was an average of 87 deaths per year from lightning. Curran et al. also rank the state of Texas as third in the number of fatalities from 1959 to 1994, behind Florida at number one and North Carolina at number two (Curran et al. 2000).

There is an obvious need for the protection of life and property from lightning flashes to ground. While protection of a structure from lightning can be found in the use of a lightning rod, protection to life can be found in the forewarning or "forecasting" of lightning strikes coming to ground. One step in this direction was the development of lightning detection systems that began in specific regions of the United States (Krider et al. 1980; Orville et al. 1983, 1987) and grew into the development of the National

---

This thesis follows the style of *Monthly Weather Review.*

Lightning Detection Network (NLDN) (Orville 1991; Orville and Huffines 2001) and then the North American Lightning Detection Network (NALDN) (Orville et al. 2002). This dataset can be used along with the developing Time of Arrival (TOA) networks that include the Lightning Detection and Ranging (LDAR) networks over Kennedy Space Center (KSC), Dallas / Ft. Worth (DFW) and Houston, Texas (i.e. LDAR-II). The LDAR-II and NLDN networks will be discussed later.

1.2 Ordinary, Convective Thunderstorm

By definition, a thunderstorm is a cloud that produces thunder (MacGorman and Rust 1998, p83). Therefore, one can say that a thunderstorm is a cloud that produces lightning. Several classifications of thunderstorms exist and are classified by their visual appearance on radar and their longevity and severity. Weisman and Klemp (1986) break the types of convective storms into 3 categories: the short-lived single cell, the multicell, and the supercell. Weisman and Klemp (1982, 1984) show with conceptual models that convective storm type depends on vertical wind shear and buoyancy, with small magnitudes of vertical wind shear likely to produce ordinary, convective storms. Weisman and Klemp (1986) describe the short-lived single cell storm as the most basic convective storm. Therefore, this ordinary convective storm type will be the focus of this study.

This storm type consists of a single updraft that rises rapidly through the troposphere and produces large amounts of liquid water and ice. A downdraft is created when cloud or ice particles become too heavy for the updraft to support. Intracloud (IC)

lightning (discussed later) dominates in early stages of convective activity and is correlated with the vertical development of the cloud, growth of ice crystals, and radar reflectivity above the inferred negative charge region (Williams et al. 1989). This storm type, as said before exists in a low shear environment, will then begin to dissipate during the downdraft process due to the lack of dynamical support.

1.2.1 Cumulus Stage

Byers and Braham (1949) found this storm type to have three distinct stages (Fig. 1). The first stage, known as the cumulus stage (Fig. 1a), is characterized by an updraft throughout the cell. The origin of this stage is simply a cumulus cloud developing in an unstable environment. In its early development, this stage is not detected by radar, but can be seen by the naked eye as a towering cloud rapidly growing in vertical extent. Tuttle et al. (1989) state that the initial stages of thunderstorm development are dominated by collision – coalescence growth processes. While in this stage, the cloud may grow until its visible top exceeds the height where the temperature is -30°C or colder (Byers and Braham 1949). The initial stage duration is between 10 and 15 minutes, however, it is difficult to determine an exact time duration since it begins with the initial appearance of the cumulus cloud that becomes the thunderstorm cell (Byers and Braham 1949). Using the Florida LDAR system, Lhermitte and Krehbiel (1979) indicate that up to 15 intracloud flashes can precede the first cloud-to-ground (CG) flash in this initial stage of thunderstorm development.

1.2.2 Mature Stage

The second stage of thunderstorm development is the mature stage and is characterized by the presence of both updrafts and downdrafts, at least in the lower half of the cell (Fig. 1b). With the continued updraft, more vapor condenses and the drops and ice crystals within the cloud become larger and more numerous. As the storm intensifies, growth by accretion – freezing becomes the dominant growth mechanism (Tuttle et al. 1989). As mentioned before, a downdraft begins when the updraft can no longer support these growing droplets and ice crystals and they begin to fall towards the earth. According to Byers and Braham (1949), the identifying characteristic in which the cumulus stage transitions to the mature stage is the occurrence of rain at the surface of the earth. The structure of the mature stage is marked by the position of the downdraft adjacent to the continuing portion of the updraft. Involved in the formation of the downdraft is the drag on the ascending air by the precipitation, which is falling towards the earth. The moving air created by the downdraft, when coming into contact with the ground, spreads out horizontally and creates a phenomenon known as an outflow boundary or gust front (Byers and Braham 1949). Along with the sharp increase in wind speed and direction at the surface, this gust front also decreases the surface air temperature significantly. It is important to note that hail occurs in the mature stage,

although it is not necessarily found in every storm. The end of the mature stage is identified when the downdraft area in the lower levels of the storm increases in size until it extends over the entire storm cell. The duration of the mature stage is usually 15 to 30 minutes (Byers and Braham 1949).

1.2.3 Dissipating Stage

The third and final stage of a thunderstorm cell is the dissipating stage (Fig. 1c). It is characterized by weak downdrafts prevailing throughout the cell (Byers and Braham 1949). This process continues until the entire vertical and horizontal extent of the cell only contains downdraft. As one would assume, precipitation at the surface within the dissipating stage diminishes until the last drops have fallen from the cell. Byers and Braham (1949) note that this precipitation minimum may occur up to 20 – 30 min. after the significant vertical motion in the cell stops. The end of the dissipating stage, therefore, is marked by the cessation of precipitation and the distortion of the surface wind field by the cell is no longer apparent. The typical time duration of this "airmass" thunderstorm is on the order of 45 – 75 min. (Byers and Braham 1949).

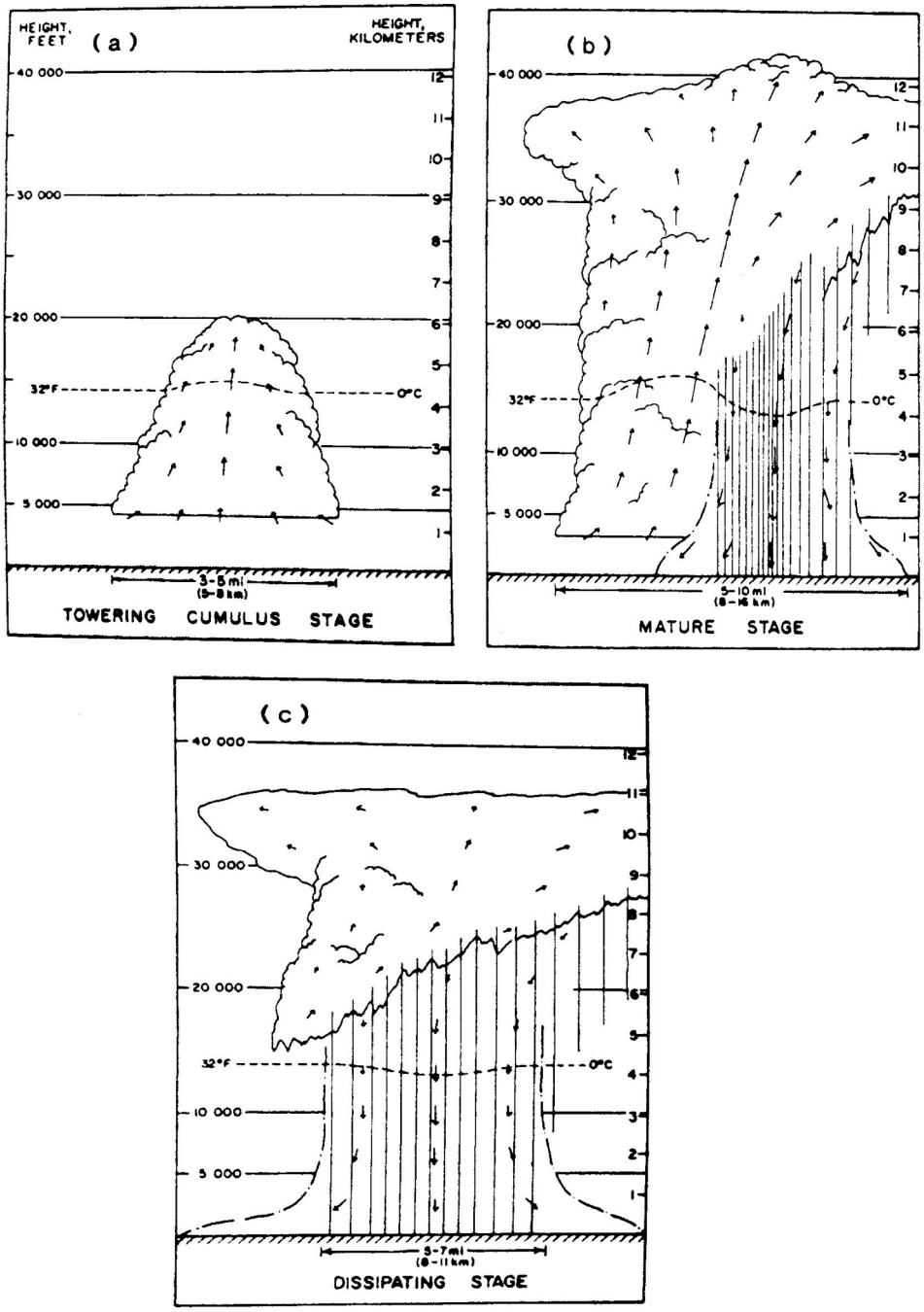

Fig. 1. Stages of development of an ordinary, convective thunderstorm. Cumulus stage (a), mature stage (b), and dissipating stage (c) as first described by Byers and Braham (1949) (Adapted from Ray 1986, p. 333).

1.3 Thunderstorm Charge Structure

The primary source of lightning is electric charge separated in a cloud type known as a cumulonimbus (Cb) (Uman 1987). However, according to Imyanitov et al. (1971), not every Cb produces lightning. Electrified thunderstorms interact with upper-atmospheric regions (e.g. the electrosphere) and maintain what is known as the global electrical circuit (Fig. 2).

Interactions between different types of hydrometeors within a cloud are thought to carry or transfer charges, thus creating net charge regions throughout a thunderstorm. Charge separation can either come about by inductive mechanisms (i.e. requires an electric field to induce charge on the surface of the hydrometeor) or non-inductive mechanisms (i.e. do not require hydrometeors to be polarized by the ambient electric field) (e.g., Takahashi 1978). MacGorman and Rust (1998, p. 56-70) describe several theories that exist to explain how charge can be placed on hydrometeors and how differing charge regions develop.

As mentioned before, lightning results from charge separation within a thunderstorm. This charge structure of a thunderstorm was first thought to be of a positive dipole with a positive charge region above a negative charge region (e.g., Wilson 1916, 1920, 1929). These findings led to numerous electric field studies of thunderstorms. Some researchers claimed that the lowest charge in thunderstorms was positive, thus maintaining that a negative dipole thunderstorm charge structure existed (MacGorman and Rust 1998, p. 50).

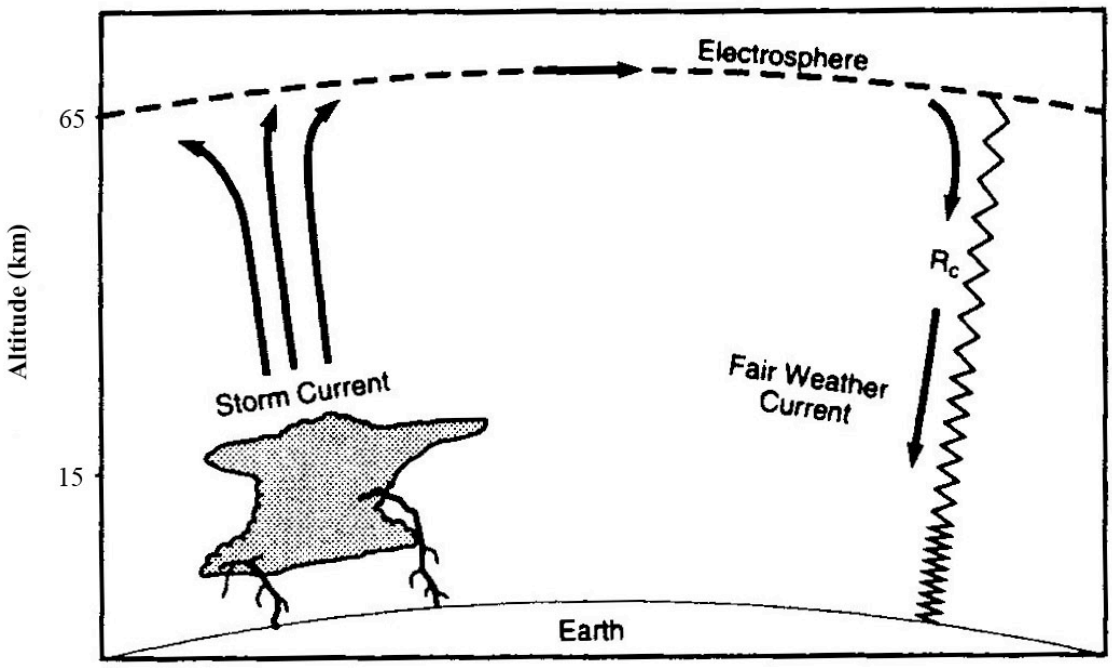

Fig. 2. Electrified thunderstorms interact with upper-atmospheric regions and maintain what is known as the global electrical circuit. The thunderstorm is effectively a battery, charging the earth's surface with negative charge lowered due to lightning discharges. Altitudes are not to scale (From MacGorman and Rust 1998, p. 31).

To determine the solution more directly, Simpson and Scrase (1937) and Simpson and Robinson (1941) launched balloons into thunderstorms to measure the corona caused by the vertical component of the electric field. They found that thunderstorms do contain a positive dipole. However, it is insufficient to only use the "two charge" model as they discovered a third, smaller positive charge that exists below the main negative charge in many storms (Fig. 3). This gross charge structure of a thunderstorm is often labeled a dipole/tripole structure (MacGorman and Rust 1998, p. 50). It is important to note that actual thunderstorm charge distributions are usually more complex than the conceptual dipole/tripole as found from these storm measurements (e.g., Moore and Vonnegut 1977; Krehbiel 1986).

MacGorman and Rust (1998, p. 52) highlight the typical characteristics of the overall charge structure of thunderstorms. Negative charge usually dominates the lower portion of the thunderstorm. Temperatures within this charge region are slightly warmer than -25°C and sometimes warmer than -10°C. Another common characteristic is a positive region that lies 1 km above this negative charge region and net positive charge dominates the upper region of thunderstorms and in their anvils (e.g., Gish and Wait 1950). *In situ* measurements also confirm that differing charge regions are not only stacked vertically but vary horizontally as well. This evidence further complicates our knowledge of the charge structure of a thunderstorm.

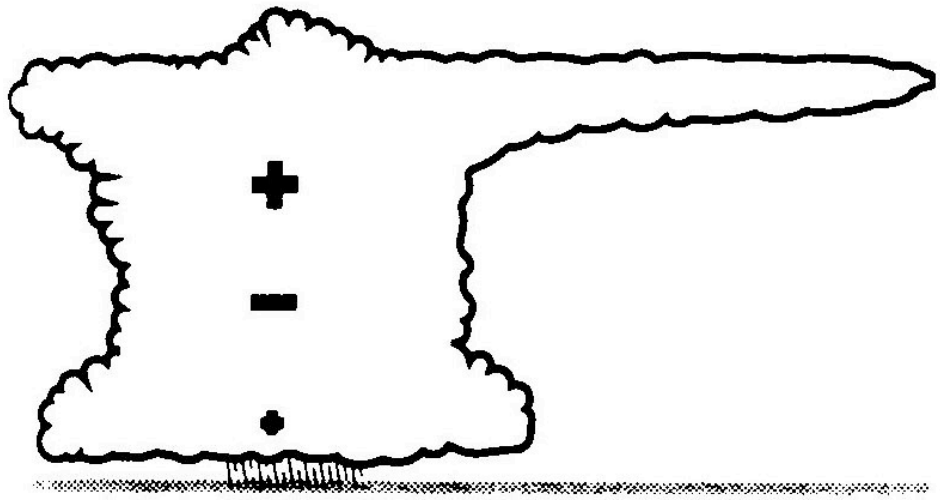

Fig. 3. Positive dipole or tripole charge structure of a thunderstorm as derived from Simpson and colleagues. Thunderstorms might often resemble a more complicated storm structure than depicted (From MacGorman and Rust 1998, p. 51).

1.4 Fundamentals of Lightning

1.4.1 Cloud-to-ground Lightning

CG lightning is an electrical discharge that occurs between the thunderstorm and the earth (Uman 1971, p. 65). It is important to note that the entire lightning discharge or event is termed a "flash" and has time duration on the order of a half second. A flash is comprised of several smaller discharges, each known as a "stroke". Each stroke lasts over a millisecond (Uman 1987, p. 10). The following CG lightning summary is adapted from Uman (1971, 1987) and is illustrated in Fig. 4. CG lightning occurs when charge separation processes produce a potential difference between differing charge regions within a thunderstorm. Once the electrical breakdown field strength is reached, a

preliminary breakdown occurs between the main negative charge region and the lower positive charge region (i.e., Fig. 3). This breakdown leads to the initiation of a stepped leader. The stepped leader is a discharge that moves downward in discrete steps that are on the order of 10s of meters in length. The stepped leader tends to branch in a downward direction while inducing a charge on the surface of the earth.

As the tip of the bottom leader nears the ground, the electric field at the ground exceeds the breakdown value of air and one or more discharges propagate upwards from the ground. These upward propagating discharges are known as streamers. During the attachment process, the upward streamer (opposite in polarity than the stepped leader) meets the stepped leader at a junction point that is some tens of meters above the ground. The leader channel is then discharged when the first return stroke propagates continuously up the previously charged leader path. As the return stroke moves upwards, large numbers of electrons flow downward from greater and greater heights up in the lightning channel. The return stroke lowers the net charge available in the leader channel as well as the charge available at the top of the channel. Visibly speaking, the return stroke is the bright, luminous channel that is seen by the naked eye. The rapid release of energy during the return stroke process heats the lightning channel to a temperature near 30,000 K. This temperature increase generates a high-pressure shock wave, which eventually becomes thunder. If the return stroke current ceases here, the lightning discharge is known as a single stroke CG flash.

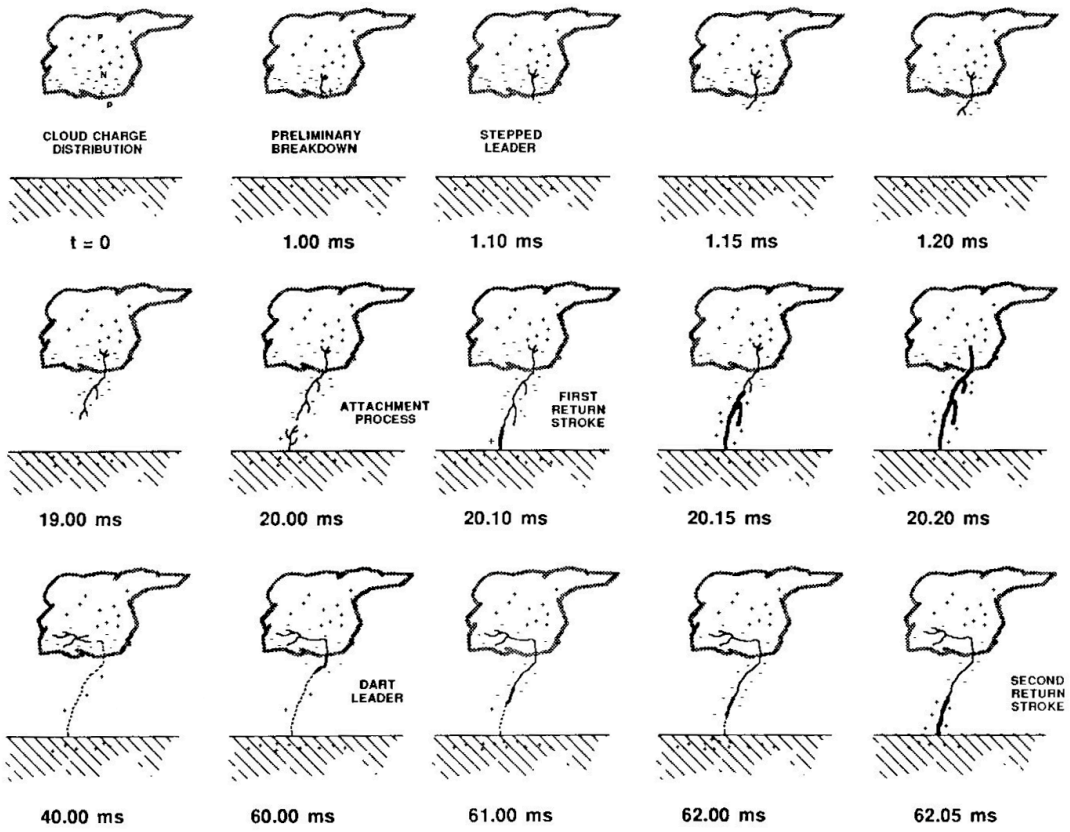

Fig. 4. A conceptual drawing of the various processes of a downward negative lightning flash (From Uman 1987, p. 12).

If additional charge is still available at the top of the channel, a continuous leader, or dart leader, develops and moves down the previous lightning channel. The dart leader then begins the subsequent return stroke (or third, etc.). One difference between the stepped leader and the dart leader is that the dart leader is not branched because the stepped leader has already established the lightning channel. However, if the time interval between the return stroke and the dart leader is greater than 100 msec, the dart leader will start a new path and become a stepped leader. Most lightning flashes contain three to five strokes, however, Kitagawa et al. (1962) recorded a flash that contained 26 strokes in a thunderstorm in New Mexico.

CG lightning flashes can occur with either negative polarity or positive polarity. Therefore, depending on the type, negative or positive charge is transported to the ground through the lightning channel. According to Berger (1978), the downward moving negatively charged leader accounts for 90% or more of global cloud-to-ground lightning where the remaining 10% or less of CG discharges are downward positive lightning flashes.

1.4.2 Intracloud Lightning

Lightning discharges that remain within the thunderstorm (i.e., never come in contact with the ground) and connect two regions of opposite charge are known as intracloud flashes (IC). Each CG lightning flash has an intracloud discharge associated with it. Rakov and Uman (2003, p. 321) state that approximately 75% of lightning discharges do not come to ground. Livingston and Krider (1978) found in summer thunderstorms over Florida that between 42 and 52 percent of all lightning discharges were CG during the active storm period. Approximately 20% were CG during the final storm period of each of their cases.

The typical IC discharge is thought to take place between the upper positive region and the main negative region as shown in Fig. 3 (Uman 1971, p. 68). Uman goes on to say that the time duration, charge transfer, and length of an IC flash is similar to that of a CG discharge, however, the discharge processes vary because of the differing environments in which they occur. CG lightning discharges onto a conductor (i.e., the earth), whereas the IC discharge does not. The typical IC discharge is essentially made up of a slowly moving spark or leader, as contrasted to the discrete strokes that make up a CG flash (Uman 1971, p. 69). According to Uman (1987, p. 21), subsequent return strokes (or recoil streamers) are then generated when the leader contacts areas of space charge of opposite sign. The continuous luminosity observed in the cloud occurs during the leader propagation along with numerous short luminous pulses that last about a thousandth of a second (Uman 1971, p. 70).

Controversy exists in knowing whether or not the leader moves up from the main negative region and carries negative charge or moves down from the upper positive region and carries positive charge. Uman (1971, p. 69) suggests that each may occur on different occasions. It is important to note that much more is known about CG lightning than IC lightning, primarily due to the fact that IC lightning channels are hidden by the cloud and cannot be photographed. However, with the developing LDAR-II networks, scientists are now learning more about intracloud lightning.

1.5 Previous Studies and Hypothesis

Prior studies have developed techniques to predict the onset of cloud-to-ground lightning flashes using various operational tools, primarily the use of the Weather Surveillance Radar 1988-Doppler (WSR-88D). Dye et al. (1989) determined that lightning would occur when the 40-dBZ echo reached the -10°C temperature height when studying small thunderstorms in central New Mexico. Buechler and Goodman (1990), while studying storms in New Mexico, Alabama, and Florida, identified storms as having lightning if the 40-dBZ echo reached the -10°C isotherm and the echo tops exceeded 9 km. Michimoto (1991) used the criteria of the 30-dBZ echo at the -20°C temperature height and observed that the first CG flash occurred 5 min. after a storm in the Hokuriku District of Japan reached this criteria. Gremillion and Orville (1999) found from analyzing reflectivity data of 39 airmass thunderstorms over KSC that the 40-dBZ echo detected at the -10°C temperature height was the best indicator for predicting the

initiation of CG lightning. The median time lag between their Lightning Initiation Signature (i.e., aforementioned reflectivity threshold achieved for two consecutive volume scans) and the first CG was 7.5 minutes. A 15 minute median time difference between the first 10-dBZ echo aloft and the first detected CG lightning strike was found by Hondl and Eilts (1994) when studying 28 thunderstorms over central Florida. However, the range of CG lead times varied from 5 to 45 minutes! Vincent et al. (2004) used several characteristics of WSR-88D data to determine the best lightning prediction algorithm of storms in North Carolina. Characteristics included a reflectivity threshold at a certain environmental temperature height for a specified number of radar volume scans. According to this study, the best predictor of CG onset was the initiation of 40-dBZ at -10°C for one volume scan. This "combination" had a 37% false alarm rate (FAR), a 100% probability of detection (POD) and 63% critical success index (CSI) with an average CG lead time of 14.7 min. (Vincent et al. 2004). Conversely, a minimal number of studies have employed the use of total lightning detection systems (e.g., LDAR) to predict the onset of CG lightning in convective activity. In 13 cases over Houston, Motley (2006) found that the first CG flash occurred at an average of 12 minutes after the first IC flash.

According to Williams et al. (1989), 10 or more cloud flashes may occur before the first CG flash. Therefore, we hypothesize that the real-time detection of total lightning can be used as a forecasting tool in forewarning the public of the subsequent cloud-to-ground lightning dangers. This study will examine the possible correlation between the first detected intracloud lightning flash and the first NLDN detected cloud-

to-ground discharge in 37 isolated, ordinary thunderstorms over Houston, Texas. This study will also incorporate the various radar parameters mentioned above so that forecasters in the Houston area can have several methods to aid in forecasting the onset of CG flashes. This information can possibly lead to the real-time forecasting of CG lightning within the city of Houston and can be used as motivation for future studies within other cities across the United States.

Several observational characteristics of the 37 cases will be described in this study, such as total flash rates of each storm along with the time duration of the total flashes and CG flashes alone. Also, percent positive flash statistics will be presented and compared to other studies that focused on the same geographic region. In addition to finding the "best" predictor to the onset of CG lightning, examination of the various operational methods will attempt to find a radar or lightning signature that forecasters can use to predict the complete cessation of CG lightning in each thunderstorm event. Within the confines of this study, we hope to provide valuable information to forecasters within and around the Houston area, in order to prevent future lightning related injuries and fatalities.

2. DATA AND METHODOLOGY

2.1 Lightning Detection and Ranging

The LDAR-II (hereafter, referred to LDAR) system over Houston, Texas is able to map lightning discharges in three dimensions, therefore illustrating the total lightning structure of any thunderstorm event in detail. This LDAR network consists of twelve very high frequency (VHF) time-of-arrival (TOA) sensors that were purchased from Vaisala Inc. and installed by the Texas A&M Department of Atmospheric Sciences and has been in operation since August 2005 (Fig. 5) (Ely et al. 2007). The Houston LDAR is based on the original LDAR system developed at NASA's Kennedy Space Center (e.g., Lennon and Maier 1991).

TOA systems map lightning in three dimensions by detecting short pulses of VHF radiation (also known as VHF sources). These pulses are modeled by accurately measuring their time of arrival at several sensors (i.e. assuming VHF signals propagate along line-of-sight) (Ely et al. 2007). Precise timing of the network is accomplished by incorporating Global Positioning Satellite (GPS) technology into each sensor. Each sensor records the time and signal power of the largest amplitude pulse during a 100 μs interval, therefore, giving the network the capability to detect a maximum of 10,000 sources per second (Ely et al. 2007).

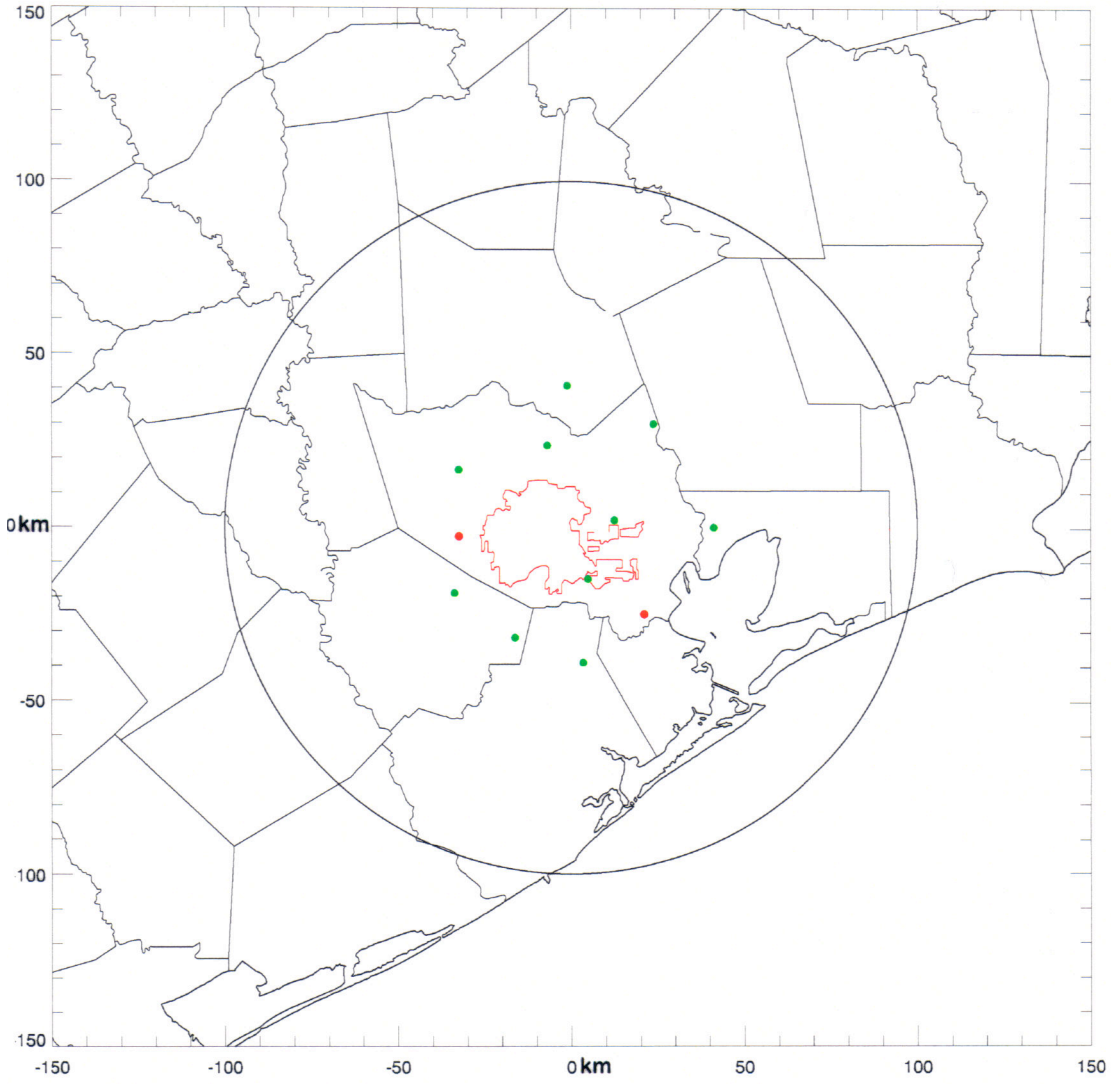

Fig. 5. Map depicting the locations of the twelve TOA sensors that make up Texas A&M University's LDAR network over Houston, Texas. The green dots represent the 10 sensors that were operational during this study and the red dots are sensors that are currently installed, but were not operational during this study. The black circle is a 100 km range ring centered about the LDAR center. The red outline in the center is the city boundary of Houston and some surrounding industrial cities.

According to MacGorman and Rust (1998, p. 161), when a pair of TOA stations sense a specific VHF source, the time difference between its arrival at each sensor is calculated. A locus of constant time difference is then defined, which is a hyperbola that passes through the VHF source location. Using a third station, a second hyperbola of constant time difference is calculated that intersects the first hyperbola at the point where the VHF source occurred (Fig. 6). MacGorman and Rust caution readers by stating that using only 3 stations could result in two plausible flash locations in some regions. Therefore, a fourth station is required to eliminate this possibility. The LDAR network requires that a minimum of 5 stations be operational to record the time of arrival of a VHF source to improve the accuracy of the VHF source location.

Limitations do exist within the LDAR network, primarily with regard to detection efficiency and effective range. Based on the case study of a mesoscale convective system (MCS) over Houston on 31 October 2005, Ely et al. (2007) found the effective range of the network to be 120 – 130 km from the LDAR network center. They also found a median 3D location error of 250 m or better for VHF sources that originate at 3 km or higher in altitude and a location accuracy of 1 km at a distance of 100 km from the LDAR center. Similar to their study, all analyses presented in this study do not extend beyond a range of 100 km from the LDAR center.

LDAR data are transmitted from each sensor in real-time to Texas A&M and each sensor is capable of storing the data to hard disk at its site. These archived data are then collected every other month and processed to provide the highest quality dataset for research analysis (Ely et al. 2007). Therefore, total lightning (i.e. intracloud flashes and

incloud components of CG flashes) data were collected for each convective case in this study.

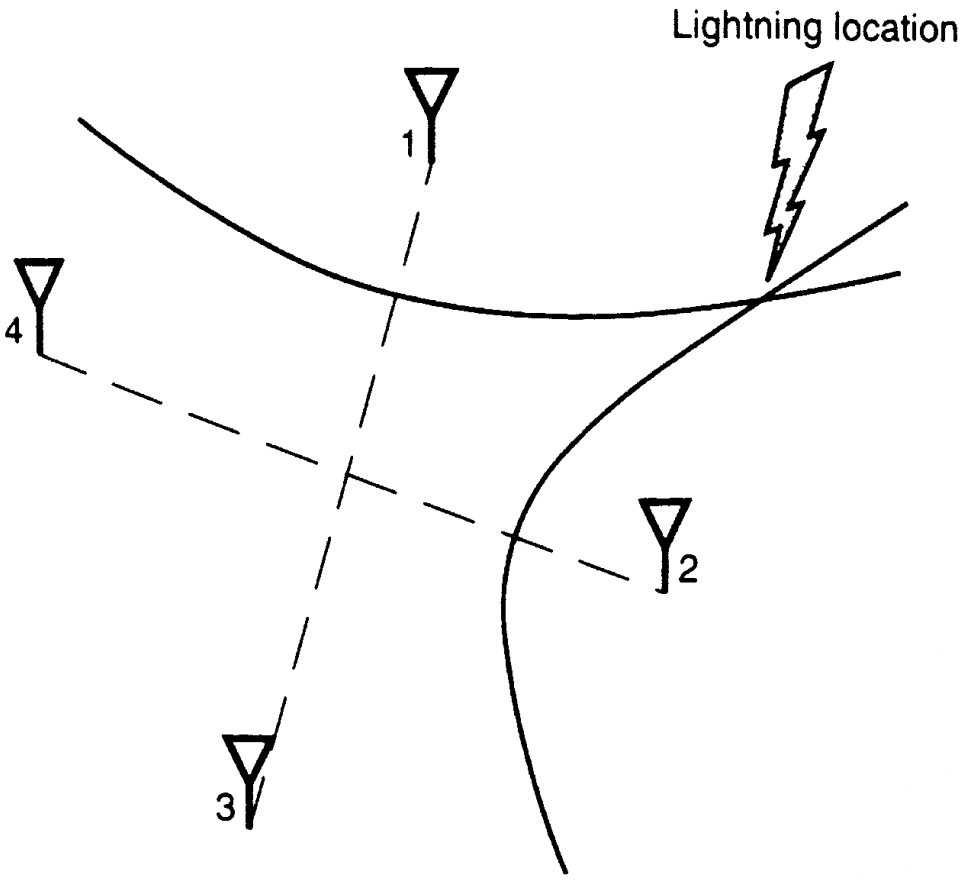

Fig. 6. Location of a ground strike as detected by a time of arrival system. The intersection of the two hyperbolas designates the location of the lightning channel (From MacGorman and Rust 1998, p. 161).

The Total Electrification Display (TED) (Fig. 7) was used to determine if a particular thunderstorm event contained lightning. TED is an interactive program that displays total lightning data from the LDAR network in real-time. However, beneficial to this study is its ability to display archived total lightning data. TED allows the user to view VHF sources (displayed as point sources) in plan view (X-distance vs. Y-distance) (Fig. 7d), in X-distance vs. height (km) view (Fig. 7b), and in height (km) vs. Y-distance (Fig. 7e). Also included in its display is a time versus height panel (Fig. 7a) that groups VHF sources together into flashes based on their spatial and temporal characteristics. Fig. 7c is a histogram that calculates the frequency of VHF source occurrence with height. VHF sources are assigned colors based on their exact time, with older sources receiving "cold" colors (i.e. purples and blues) and newer sources receiving "warm" colors (i.e. yellows and reds). Therefore, TED gives the user the exact time and location (X, Y, height) of each VHF source. Currently, TED is unable to display cloud-to-ground lightning, thus only being used for its intracloud lightning display.

2.2 National Lightning Detection Network

The National Lightning Detection Network (NLDN), using IMPACT-ESP (IMProved Accuracy from Combined Technology) sensors with direction finder (DF) (e.g., Krider et al. 1980) and TOA technologies (Cummins et al. 2006), is used across the United States to detect the occurrence of cloud-to-ground lightning flashes in real-time. Orville et al. (2002) describe the NALDN to consist of the 187 sensors from both the

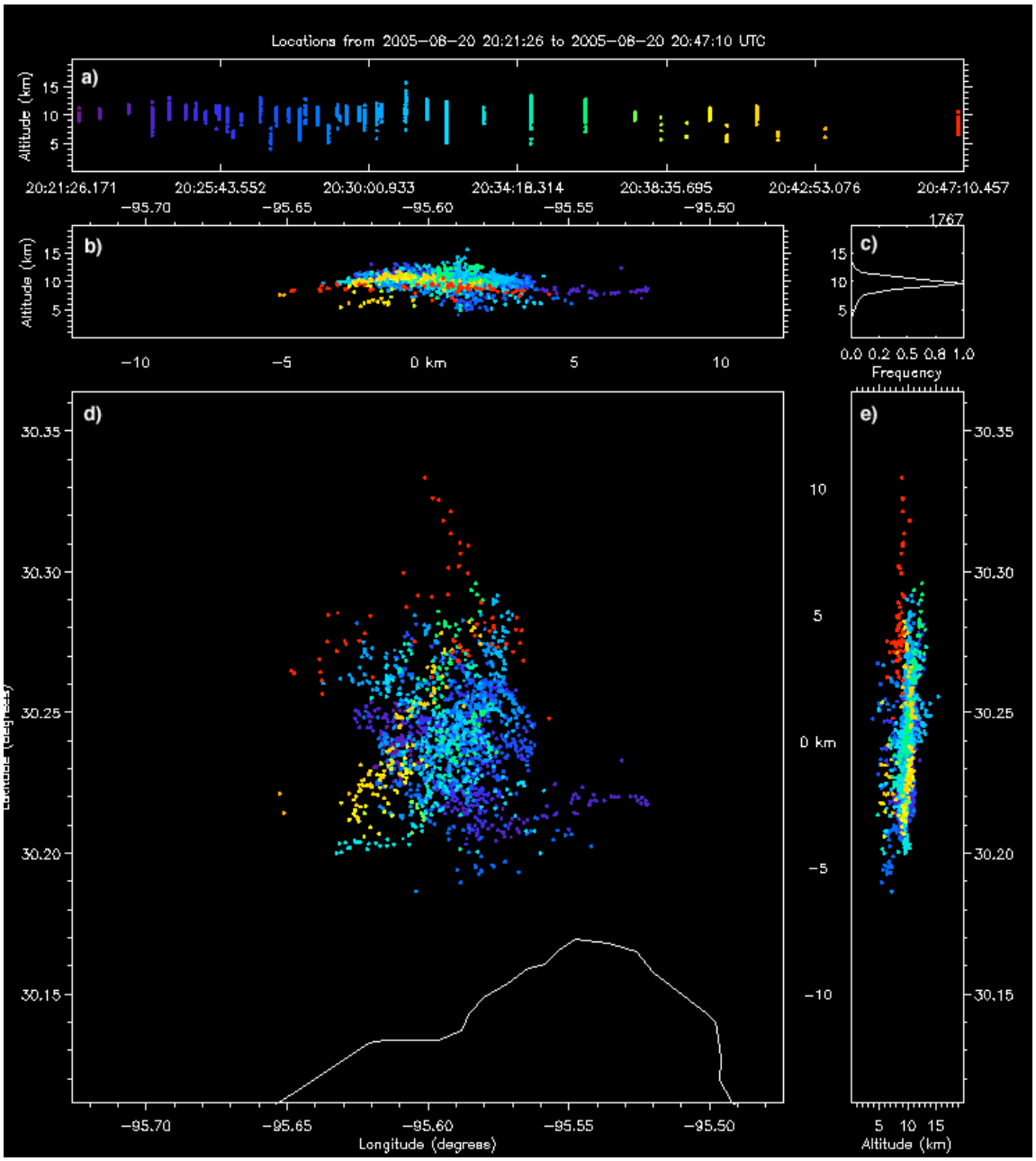

Fig. 7. Total Electrification Display (TED) displaying VHF sources from a thunderstorm event on 20 August 2005. (a) Time vs. height (km) plot in which VHF sources are grouped as flashes, (b) X-distance vs. height (km), (c) Histogram showing VHF source frequency of occurrence based on height (km), (d) X-distance vs. Y-distance or plan view, and (e) Height (km) vs. Y-distance.

NLDN and the Canadian Lightning Detection Network (CLDN). Cummins et al. (2006) estimate the median location accuracy of a single ground lightning discharge within the NLDN to be 500 m with estimated flash detection efficiency of 90 – 95%.

The direction finder sensor is a crossed-loop antenna that consists of two vertical loops mounted perpendicular to each other, one oriented north-south, and the other, east-west (MacGorman and Rust 1998, p. 159). The DF sensors assume the lightning channel is oriented vertically near the ground, because the magnetic field produced by a vertical channel has only an azimuthal component; the radial and vertical components are zero. Then, according to MacGorman and Rust, the signal that is induced in each vertical loop depends on the electric current in the vertical lightning channel, the range from the channel, and the cosine of the angle between the plane of the loop and a bearing to the lightning channel. When the loop points to the lightning channel, the signal produced in the loop is the maximum possible at a given range and for a given lightning current, while no signal is induced when the loop is orthogonal to the lightning channel. Using the ratio of the signals induced in two orthogonal loops, DF systems obtain a lightning signal that is independent of range and lightning current. The ratio of the signals is equivalent to the tangent of the bearing of the lightning channel. Therefore, the location of the lightning channel can be calculated by triangulating the bearings measured by two or more DF stations (Fig. 8) (MacGorman and Rust 1998, p. 160).

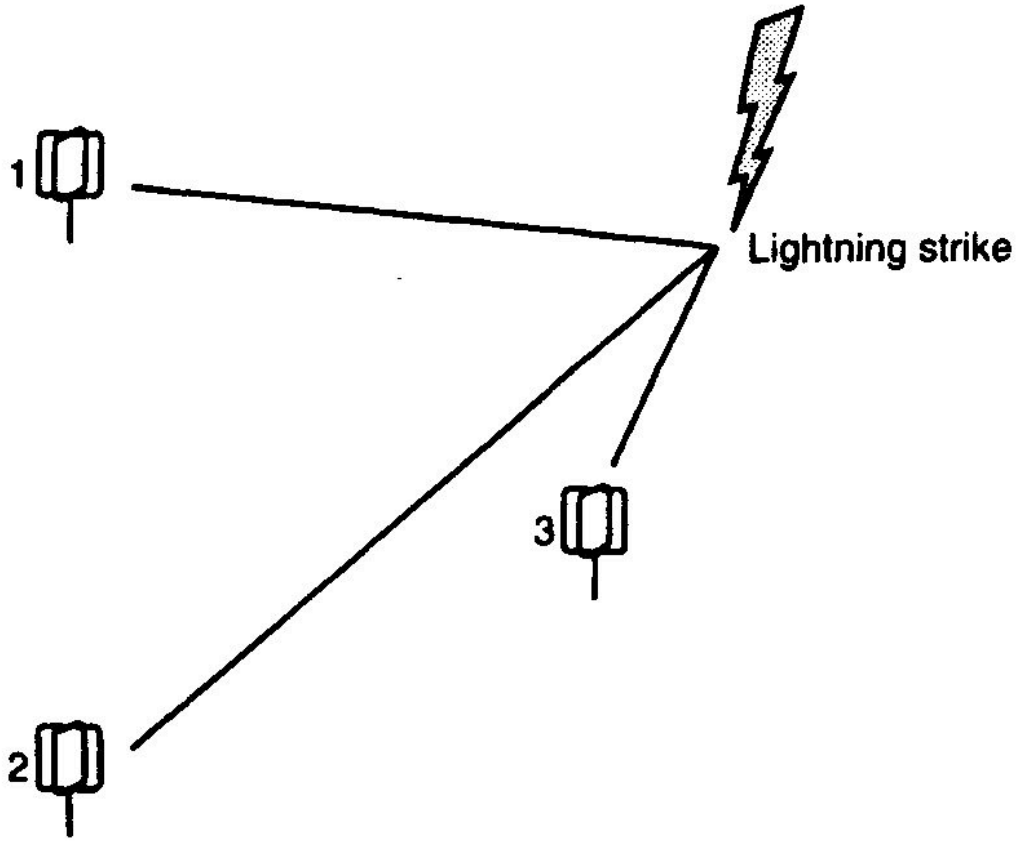

Fig. 8. Conceptual drawing of triangulating the bearing to the lightning channel measured by 3 direction finder stations. Thus, the location of the lightning strike is calculated and found (From MacGorman and Rust 1998, p. 160).

Wacker and Orville (1999) and Cummins et al. (2006) suggest the elimination from analyses the positive flashes with peak currents less than 10 kA, saying that these small positive signatures are likely in-cloud discharges. Cummins et al. go on to say that the small population of positive discharges between 10 – 20 kA are likely a mix of IC and CG discharges. For the purposes of this study, the positive discharges mentioned in the 10 – 20 kA range are counted as CG only.

The NLDN data used in this study were obtained from Vaisala Inc., Tuscon, Arizona, for the months of August and September 2005 and June and August 2006. NLDN data were available for the entire years of 2005 and 2006; however, thunderstorms only met this study's criteria during the aforementioned months (see Sec. 2.3.1 below). The NLDN data used in this study were post-processed by Vaisala Inc. such that individually detected strokes were grouped into flashes.

2.3 Radar Data

Seventeen months of WSR-88D data were examined to find 37 isolated, ordinary thunderstorms over Houston, Texas for 2005 and 2006. WSR-88D level-II data used in the detection of each event were obtained from the National Climactic Data Center (NCDC) for the radar site KHGX that is operated by the National Weather Service (NWS) Weather Forecast Office in Houston, Texas. The KHGX radar site is located southeast of Houston in League City.

The WSR-88D scanning strategy, or volume coverage pattern (VCP), that was employed during each convective event by KHGX was VCP-11 (Fig. 9). VCP-11 takes 5

min. to go through 14 elevation scans (0.5° - 19.5°) (Brown et al. 2000). Another popular scanning strategy is known as VCP-21 (Fig. 10), which only has 9 elevation scans (also 0.5° - 19.5°) and 6 min. per volume (Brown et al. 2000). For storms that extend above the 5° elevation scan, VCP-11 offers an enhanced vertical resolution than VCP-21, and according to Brown et al., VCP-11 is far superior at these heights. It is important to note that when a convective event is located within 25 km of the radar site, neither VCP detects the upper portion of the storm, thus creating what is known as a "cone of silence" (Brown et al. 2000). The cone of silence is characterized by the absence of reflectivity measurement at heights above the 19.5° elevation scan. Neither VCP does well in resolving characteristics of storm features beyond 150 km (Brown et al. 2000). Each case included in this study met both distance criteria.

Level-II data were downloaded and then analyzed using the Warning Decision Support System – Integrated Information (WDSS-II) (Fig. 11) developed by the National Severe Storms Laboratory (NSSL) in Norman, Oklahoma (Lakshmanan et al. 2007). According to Lakshmanan et al., "The individual automated algorithms that have been developed using the WDSS-II infrastructure together yield a forecasting and analysis system, providing real-time products useful in severe weather nowcasting." It is also a useful tool for post analysis of archived datasets and is used in this latter sense for this current study (Lakshmanan et al. 2007).

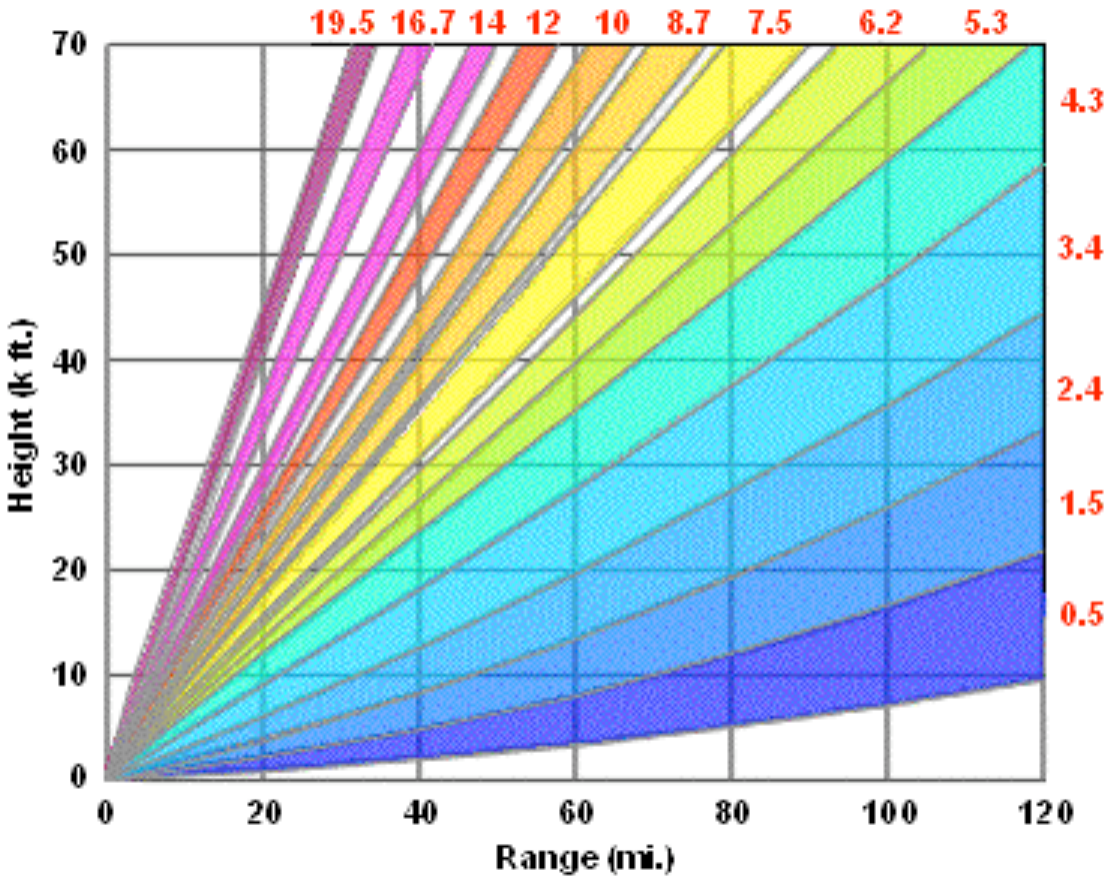

Fig. 9. WSR-88D Volume Coverage Pattern 11 (VCP-11). Scanning strategy consists of 14 elevation scans in approximately 5 minutes (From http://www.srh.noaa.gov/radar/radinfo/).

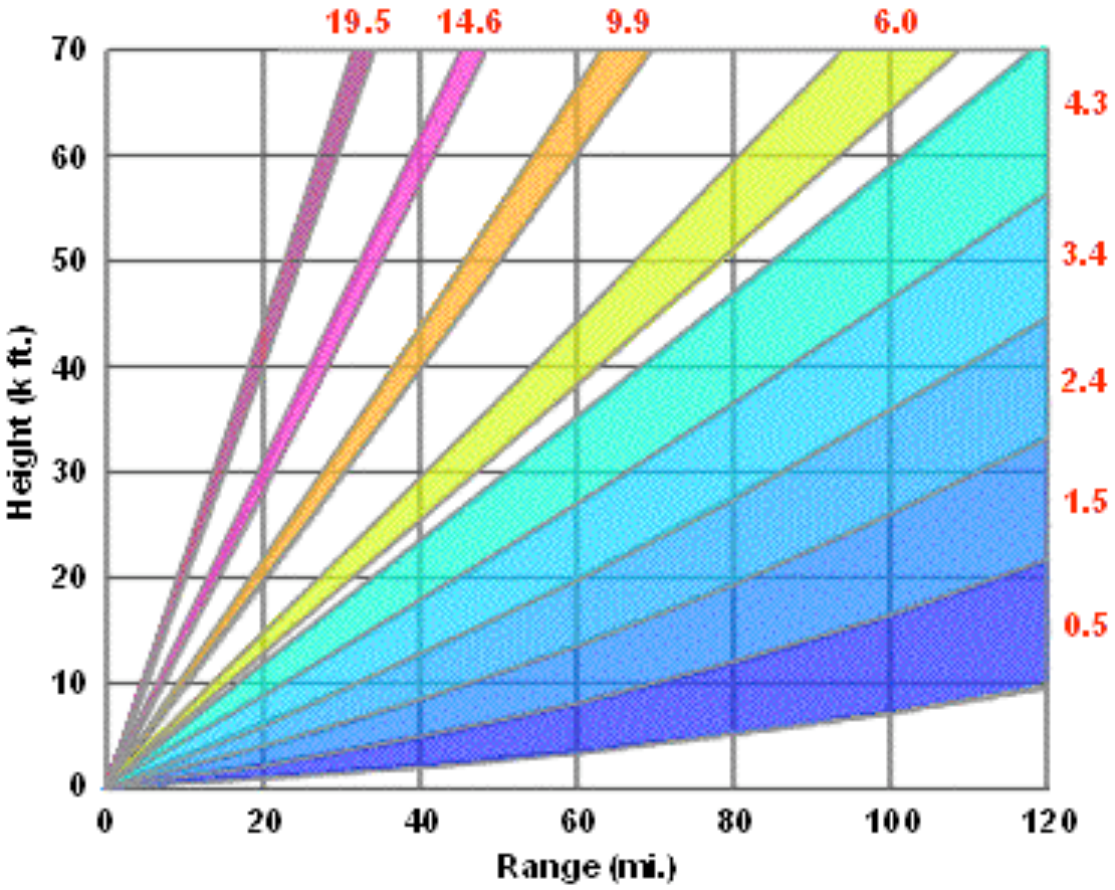

Fig. 10. WSR-88D Volume Coverage Pattern 21 (VCP-21). Scanning strategy consists of 9 elevation scans in approximately 6 minutes (From http://www.srh.noaa.gov/radar/radinfo/).

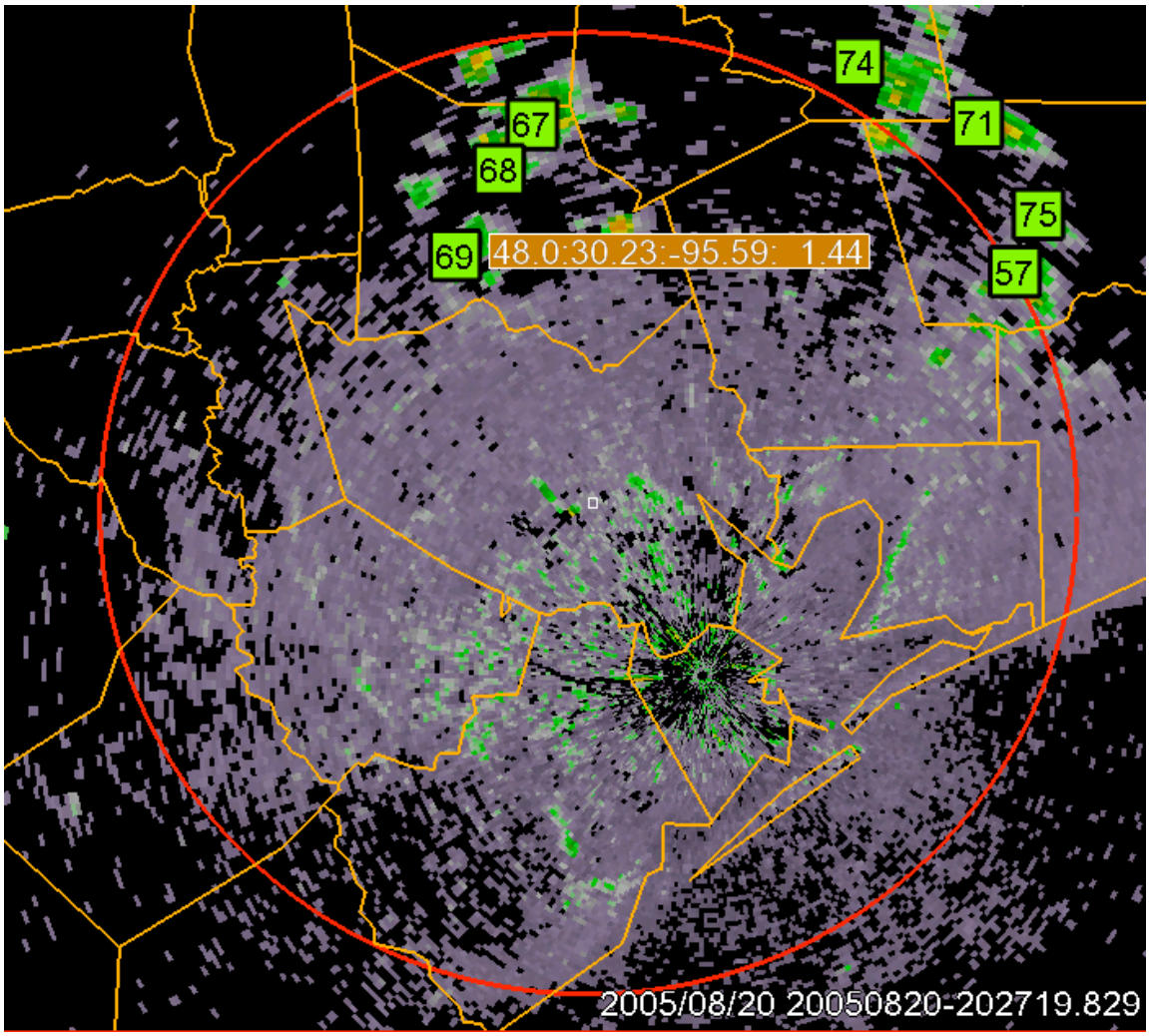

Fig. 11. WDSS-II interface displaying convective events from 20 August 2005. The green squares represent thunderstorms and their cell numbers as assigned by the SCIT algorithm. The LDAR center is represented by the small white square in the center of the image. The counties that include Houston and immediately surround the city are displayed with an orange outline. Also displayed is a 100 km range ring centered on the LDAR center as well as a text display resulting from the user's cursor over the center of cell 69. The information displayed from left to right in the text box is as follows: 48.0 is the radar reflectivity (dBZ), 30.23 is latitude (decimal degree), -95.59 is longitude (decimal degree), and 1.44 is height above MSL (km).

WDSS-II algorithms converted the level-II data from its native format to NetCDF format. A Storm-Cell Identification and Tracking (SCIT) algorithm was then run on each radar volume scan to assign a cell number specific to that cell throughout its entire lifetime. SCIT was developed due to the poor performance of the native WSR-88D storm series algorithms, especially in situations of closely spaced storms. In order to identify storms, the SCIT algorithm employs seven reflectivity thresholds as compared to the one threshold of the native WSR-88D method. According to Johnson et al. (1998), this advanced package improves the identification of storm cells. Also, because of the reflectivity criteria of the SCIT algorithm, it does not detect cells that are small, shallow or have a maximum reflectivity less than 30-dBZ (Johnson et al. 1998). Therefore, this study uses WDSS-II primarily for its display of radar reflectivity and its storm identification and tracking capabilities.

2.3.1 Thunderstorm Detection and Tracking

The combined use of the WDSS-II GUI (WG) and the Total Electrification Display (TED) aided in the detection and analysis of each thunderstorm event. Several criteria were established to objectively find ordinary thunderstorms over Houston, Texas (adapted from Motley 2006). These criteria include:

1) Storm must be identified by the SCIT algorithm for 20 minutes or longer
2) Contain VHF sources (i.e. intracloud discharges) as detected by LDAR
3) Include a minimum of at least one CG flash

4) Isolated from other convective activity as to not contain VHF sources from other storms
5) Within 100 km of the LDAR center (27.79°N and 95.31°W) (e.g., Ely et al. 2007)
6) Outside the 25 km cone of silence of the KHGX radar site (Brown et al. 2000)
7) Neither undergo a merge or split during its lifetime
8) Observed by radar during its entire lifetime

Thirty-seven storms were found to meet these criteria during the period of study between August 2005 and December 2006. Initially, storms were visually detected via radar on the WDSS-II interface. By this study's definition, storm initiation occurred when 20-dBZ was first observed around the 0°C isotherm. The complete absence of radar reflectivity at the lowest scan denoted the storm's termination. When a thunderstorm met all the above criteria during its lifetime, position and time statistics were gathered using the interactive WDSS-II GUI. The WG gives the user a mouse-over display that includes latitude and longitude coordinates (decimal degree), reflectivity values (dBZ), and height above mean sea level (MSL) (km) at any location within the bounds of a storm (Fig. 11a). The start and end time of each radar volume scan was recorded for each case, beginning with storm initiation and stopping with storm cessation. During each volume scan, the coordinates for the center of the cell are recorded. The center of each cell is defined as the visual geometric center, typically the location of highest reflectivity. Also during each volume scan, the coordinate location at any point along the cell's edge (i.e. the point where reflectivity went from positive dBZ

to zero dBZ) was recorded. Then by combining the coordinates of the cell center and visual cell boundary, a cell radius was calculated using the spherical law of cosines (available from the World Wide Web at http://www.movabletype.co.uk/scripts/LatLong.html). In trigonometry, the spherical law of cosines is a theorem that relates the sides and angles of spherical triangles (analogous to the ordinary law of cosines from plane geometry). A virtual cylinder was constructed around the bounds of each thunderstorm during each five-minute radar volume scan so that a full lightning analysis could be performed.

2.4 Analyses and Statistics Performed

2.4.1 VHF Flash Methodology

A suite of Interactive Data Language (IDL) programs was employed for the lightning analysis of the 37 isolated, ordinary thunderstorms. A local file containing the LDAR VHF source information was converted from binary format to American Standard Code for Information Interchange (ASCII) format. This ASCII file contains the exact coordinate location (i.e. latitude, longitude, and height) and precise time (up to the millisecond) of each VHF source that occurred within range of the LDAR network for a specific day. The NASA flash algorithm is used, which reads in this ASCII file and groups individual VHF sources into flashes based on certain spatial and temporal characteristics. These characteristics are based on measurements of typical flash length and propagation speed (e.g., MacGorman and Rust 1998, Ch. 5). The NASA flash

algorithm is a modified version of the algorithm used for NASA's Kennedy Space Center LDAR. The following description of the flash algorithm has been adapted from Motley (2006). The flash algorithm determines if a source was a part of a flash based on the following criteria: the maximum duration of a flash cannot exceed 3 seconds, the analyzed source is within 5 km of a source already associated with the flash, the time lag between the analyzed source and sources in the analyzed flash within 5 km is not greater than 0.5 seconds, and the maximum time delay between points in a branch cannot exceed 30 msec. A source initiates a new branch when the analyzed source is greater than 30 msec from the last source observed or if the source is greater than 5 km from the last source observed, but still within 5 km of another source in the flash. In this case, a new branch occurs to the closest source that occurred within 0.5 seconds of the analyzed source and is within 5 km of the analyzed source. If either of these conditions fails, then a new flash, rather than a new branch, is created. In addition to these characteristics, a valid flash was required to consist of at least 3 VHF sources.

Each VHF source point now has information regarding the time (day, month, year, hour, minute, second, millisecond), location (latitude, longitude, height), and location within the flash it is assigned to (flash number, position in flash, position in branch). As mentioned before, a cylinder was effectively built around each storm for every five-minute radar volume scan. This cylinder was "filled" with the VHF sources that matched the time and location of the output from the NASA flash algorithm. Checks were made with the TED GUI and an IDL program to ensure that all the VHF sources

were accurately gathered and that no flashes from other storms were included in the analyzed storm cylinder.

Additional IDL programs were employed to gather and compute the following statistics with regards to the VHF flash information obtained for each of the 37 cases: a total flash duration which is defined as the total time from when the first VHF source is detected to when the last IC flash occurs in a thunderstorm, and a total flash rate that is calculated by simply dividing the total number of flashes detected by LDAR by the total flash duration or total flash time interval.

2.4.2 Cloud-to-ground Flash Methodology

For the cloud-to-ground portion of this study, an IDL program first converted NLDN CG flash information from binary format to ASCII format. This ASCII file contains information about each ground flash that includes date, time (up to the second), location in latitude and longitude (in decimal degrees), peak current (measured in kA), and multiplicity. Similar to the aforementioned LDAR program, a program compared the time and location of CG lightning flashes to the constructed storm cylinder, therefore finding all the cloud-to-ground flashes occurring within the bounds of each thunderstorm.

Similar to the VHF flash methodology, IDL programs calculated statistics based on the CG flashes found within each convective case. For each case, a CG flash duration was calculated. This value is simply the total time between the first CG in a thunderstorm to the last occurring CG. From this, a CG flash rate is determined by dividing the total number of CG flashes within a thunderstorm by the CG flash duration.

Unlike intracloud lightning, CG flashes can either carry positive or negative charge to ground. Therefore, percent positive flash occurrence will be calculated for each event in this study and compared to those of previous studies.

The time separation between the first VHF source and the first CG lightning flash also calculated for each thunderstorm case. Also investigated was the occurrence of the last lightning flash for each event and its classification as either a CG or IC.

2.4.3 Radar Methodology

Using the WDSS-II GUI, each thunderstorm case was analyzed to find the time at which the 30-dBZ and 40-dBZ radar echo first reached the -10°C isotherm (see Sec 1.5). The environmental -10° C height over Houston was calculated by first linearly interpolating the 1200 Z sounding from the Lake Charles (KLCH) and Corpus Christi (KCRP) rawinsonde sites for each day that a convective event occurred. Then, using the values obtained from both soundings, the -10°C height over Houston was found using a weighted average based on its spatial distance between Corpus Christi and Lake Charles.

Convective cells were then analyzed using the WDSS-II display. Its mouse-over read-out that includes reflectivity and height above MSL (Fig. 11a) was used to determine what the reflectivity of a convective cell was at the height of the -10°C isotherm. Since the height of the -10°C isotherm was rarely observed directly on the PPI elevation angle display, interpolation between two different radar elevation tilts had to be performed (e.g., Vincent et al. 2004). This interpolation was performed by examining

the reflectivity of the scan below and above the -10° C isotherm heights and recording the corresponding height and reflectivity values for each cell. However, prior to interpolation, the reflectivity value for each scan was first converted from its logarithmic form:

$$Z = 10\log_{10}\left(\frac{z}{1mm^{6}m^{-3}}\right) \quad (1)$$

to its linear form:

$$z = 10^{\left(\frac{Z}{10}\right)} \quad (2)$$

After the interpolation was performed, the radar reflectivity was converted back to its logarithmic form.

The time stamp of the radar volume scan at which the 30-dBZ and 40-dBZ echoes first reached the -10°C isotherm is recorded and compared to when the first CG comes to ground in each thunderstorm case. These radar signatures will also be compared to when the first VHF source was detected in each case. A comparison can then be made between a radar-induced warning time to CG activity and a warning time base solely on lightning data.

Radar reflectivity was also analyzed using the WDSS-II interface to find an observed signature that could forewarn when the last lightning flash would come to ground during each storm. While loosely observing every radar volume scan of each storm, it appeared that recording when the 50-dBZ echo last descended past either the -10°C isotherm or the 0°C isotherm would be a useful tool in predicting when the last CG would occur in this storm type. This signature was investigated by interpolating the

radar reflectivity scans below and above the aforementioned height levels. Then, the time stamp of the volume scan in which the 50-dBZ last descended past these levels was recorded. However, only a majority of the cases (roughly 65%) experienced 50-dBZ or greater at the -10°C isotherm height. Similarly, ~68% of the thunderstorm events observed 50-dBZ or greater at the freezing level.

Therefore, another approach was employed that interpolated the reflectivity value at either aforementioned height level for the radar volume scan during the last CG flash. The reflectivity at the -10°C and freezing levels was also found in the scan prior to and after the last CG scan. We hoped this approach would uncover a specific reflectivity pattern in these 3 radar volume scans (i.e. the "last CG scan", pre "last CG scan", and post "last CG scan") that could be correlated to the last occurring CG in each thunderstorm case.

3. RESULTS

3.1 General Storm Overview

Thirty-seven isolated, ordinary thunderstorms were selected for this study. Each thunderstorm exhibited the specific criteria (see Sec 2.3.1) deemed necessary for thunderstorm detection in this study. All 37 cases ended up occurring during the warm season (May – September) (e.g. Smith et al. 2005) of the years 2005 and 2006. Climatologically, ordinary convective thunderstorms or airmass thunderstorms tend to occur during the warm season when adequate heat and moisture reside along the Gulf coast region and interact with the daily sea breeze anomaly (e.g. Simpson 1994). Although lightning occurs during the cold season in Houston and along the Gulf Coast, its frequency is quite less and is brought about by a differing storm type that is typically driven by frontal features. Huff and Changnon (1973) found an 8% increase in non-frontal rainfall during the warm season and a 17% increase during June – August within the city of Houston for 1964-8. From Fig. 12 and Fig. 13, one can see the difference in magnitude of the average cloud-to-ground flash density between the winter months (December - February) and the warm season (May – September) over Houston. The peak in average flash density just east of Houston is 0.75 flashes km^{-2} during the winter months (Fig. 12) and between 5-7 flashes km^{-2} during the warm season (Fig. 13).

While each event in this current study is of the same storm type, moderate variability existed between each case. The variability in each statistic calculated will be noted in the following sections.

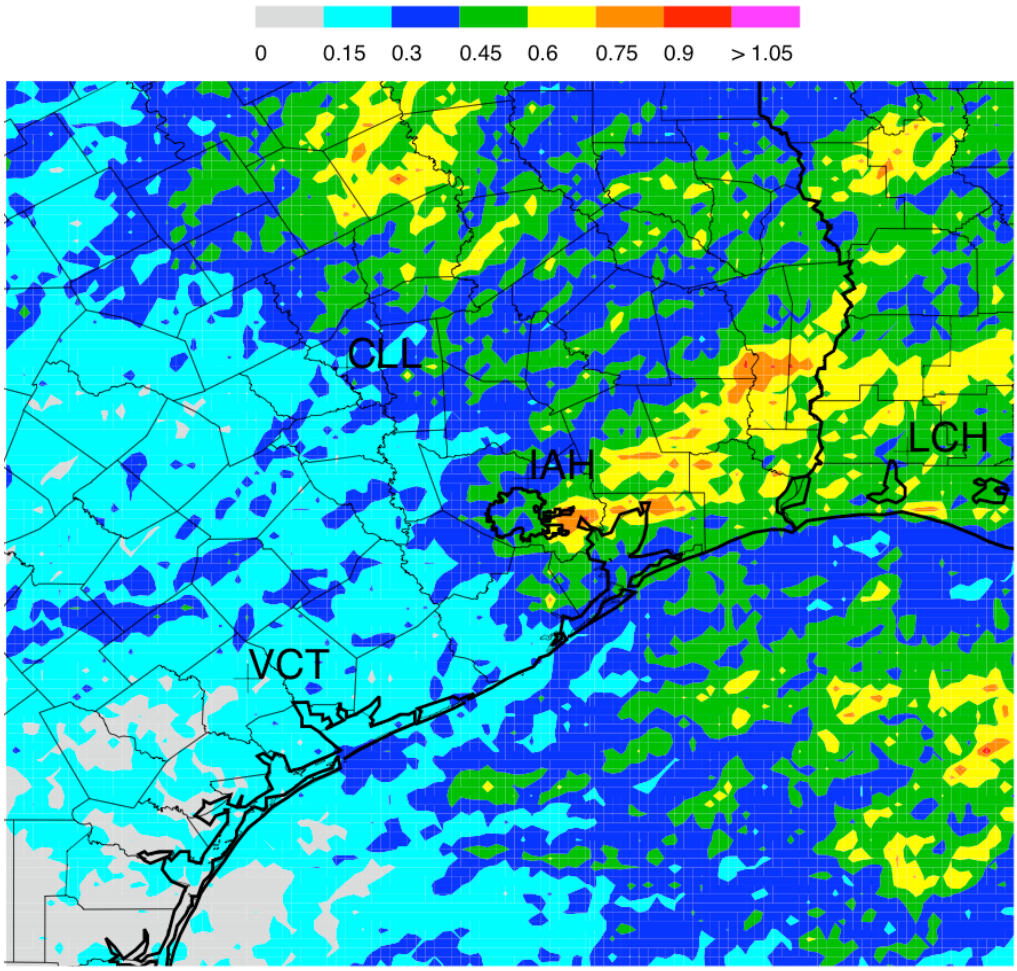

Fig. 12. 1996 – 2005 mean cloud-to-ground flash density (flashes km^{-2}) for the winter months of December – February. Houston is outlined in dark black and marked by George Bush Intercontinental/Houston Airport (IAH). Cities also shown are Victoria (VCT), College Station (CLL), and Lake Charles, Louisiana (LCH).

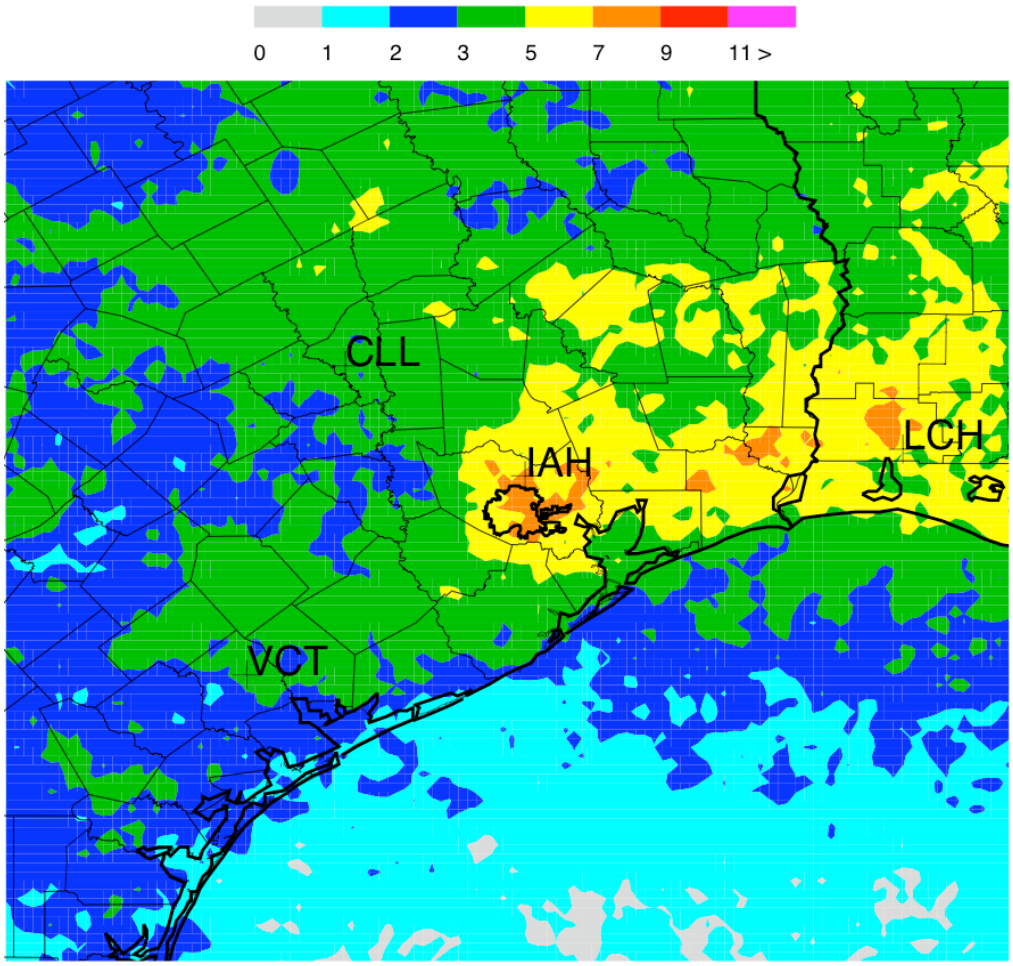

Fig. 13. 1996 – 2005 mean cloud-to-ground flash density (flashes km^{-2}) for the warm season (May - September). Houston is outlined in dark black and marked by George Bush Intercontinental/Houston Airport (IAH). Cities also shown are Victoria (VCT), College Station (CLL), and Lake Charles, Louisiana (LCH).

3.2 Warning Time for First CG and Last CG

The results of this study show the average and median time separation between the first VHF source (i.e. IC flash) and the first CG lightning discharge for 37 ordinary, convective thunderstorms over the city of Houston. For these 37 storms, the mean warning time for the first CG flash was 3.2 minutes (Table 1). The median time separation was 2.5 minutes. It is important to note that the standard deviation between each case was 3.6 minutes, thus exhibiting the variability between each case. In 3 of the 37 cases, the first CG flash preceded the first IC flash (i.e. case 1, 4, and 9). Therefore, a negative time separation value is presented for these cases. Four of the 37 cases (i.e. case 16, 26, 32, and 34) had a zero CG warning time. It was found that the first IC flash in each of these events also led to the first CG discharge. On the contrary, 8 of the 37 cases exhibited lead times greater than 5 min. while case 20 had a warning time of over 18 min. The variability from case to case can be seen in Table 1.

The average warning time to CG onset was increased by a factor of five to 16.1 minutes when using the radar reflectivity threshold of 30-dBZ at -10°C (Table 2). This time was calculated from the beginning of the radar volume scan in which the 30-dBZ echo first reached the -10°C isotherm height to when the first lightning flash came to ground. The range of CG lead times using this combination was from 4.1 min. (case 30) to 41.4 min. (case 12). In 15 of the 37 events, the 40-dBZ echo reached the -10°C isotherm during the same scan as the 30-dBZ contour. In all the other cases, the 40-dBZ echo crossed -10°C within one or two subsequent volume scans after the 30-dBZ contour scan. Therefore, the average time separation between when the 40-dBZ contour reached

Table 1. The case number (CASE #), date (mm/dd/yy), and time separation (in minutes) between the first CG flash and the first VHF source (i.e. intracloud flash) (1ST VHF TO 1ST CG) for all 37 events. Average and median warning time listed at bottom of table.

CASE #	mm/dd/yy	1ST VHF TO 1ST CG
1	08/02/05	-1.03
2	08/02/05	1.43
3	08/02/05	6.25
4	08/02/05	-0.52
5	08/02/05	0.68
6	08/03/05	3.17
7	08/14/05	1.42
8	08/14/05	3.13
9	08/14/05	-2.17
10	08/14/05	2.40
11	08/14/05	2.37
12	08/20/05	9.62
13	08/20/05	3.48
14	08/20/05	5.53
15	08/25/05	3.92
16	08/25/05	0.00
17	08/25/05	2.18
18	08/25/05	0.98
19	08/26/05	6.15
20	08/26/05	18.20
21	08/26/05	2.37
22	08/26/05	4.78
23	08/26/05	2.73
24	08/26/05	8.47
25	08/26/05	6.05
26	09/10/05	0.00
27	09/13/05	4.13
28	06/02/06	3.02
29	06/13/06	1.35
30	06/13/06	2.53
31	06/13/06	0.37
32	08/06/06	0.00
33	08/06/06	6.43
34	08/06/06	0.00
35	08/24/06	3.93
36	08/25/06	2.20
37	08/27/06	2.65
AVERAGE		**3.20**
MEDIAN		**2.53**

Table 2. The case number (CASE #) and time separation (in minutes) between the first CG flash and time at which the 30-dBZ (30-dBZ AT -10°C) and 40-dBZ (40-dBZ AT -10°C) contour crosses the -10°C isotherm for all 37 cases. Average warning time listed at bottom of table.

CASE #	30-dBZ AT -10°C	40-dBZ AT -10°C
1	5.10	5.10
2	7.27	7.27
3	14.55	9.48
4	8.08	3.02
5	6.73	6.73
6	33.25	33.25
7	16.05	10.97
8	14.72	9.63
9	12.23	7.18
10	19.60	14.55
11	12.42	7.35
12	41.38	36.32
13	9.60	9.60
14	30.32	25.23
15	15.08	15.08
16	15.52	15.52
17	22.05	22.05
18	12.08	1.92
19	31.03	15.88
20	26.57	26.57
21	24.55	9.32
22	12.42	7.35
23	17.67	12.60
24	17.45	17.45
25	9.82	9.82
26	16.03	0.93
27	15.62	5.60
28	23.27	18.38
29	5.37	0.48
30	4.10	4.10
31	6.65	6.65
32	22.32	17.53
33	17.75	12.98
34	6.37	6.37
35	16.85	11.97
36	14.68	9.73
37	12.53	12.53
AVERAGE	**16.14**	**12.07**

the -10°C height and the first CG flash was 12.1 minutes (Table 2). Variability was also present, with a range of values from 0.5 minutes (case 29) to 36.3 minutes (case 12).

The average time separation between when the 30-dBZ echo first reached the -10°C isotherm height to when first IC flash occurred was 12.9 minutes. Less than 9 minutes separated when the 40-dBZ contour reached -10°C and the first IC discharge.

Much like the observed radar characteristics employed to forewarn the onset of CG activity in a thunderstorm, several attempts were made to find a correlation for the last occurring CG in each case (see Sec 2.4.3). A 14.5 minute separation was found between when the 50-dBZ echo last descended past the -10°C isotherm height and the last CG flash. However, this signature was only observed in approximately 65% of the cases. Using the same reflectivity value at the freezing level yielded a last CG lead time of 6.6 minutes. This combination occurred in only 67% of the cases. With both of these methods, the time value is measured from the beginning of the radar volume scan in which the 50-dBZ echo is last observed at the indicated height to when the last CG flash occurred.

A more successful technique analyzed the reflectivity characteristics of the radar volume scan during the last CG flash. This radar volume scan will be referenced as the "last CG scan". The scan prior to and after the last CG scan was also analyzed. It was found when using the -10°C isotherm height as a point of reference among the three scans, the radar reflectivity fell below the 45-dBZ threshold during the last CG scan and then down to 41.7 dBZ the following scan. With reference to the freezing level, the radar reflectivity descended past the 50-dBZ threshold during the last CG scan, down from 51

dBZ during the previous scan to 47.5 dBZ in the subsequent scan. In each case, the reflectivity at either level continued to decrease in magnitude until the complete dissipation of the storm.

Based on these averaged characteristics, one can say that when the 50-dBZ echo falls below the environmental freezing level, it is likely that CG activity is terminating. However, this result is from averaging all 37 cases together. As previously mentioned, not every storm experienced 50-dBZ at 0°C. It appears to be a more valid claim that CG activity is coming to an end when the 45-dBZ echo falls below the -10°C isotherm.

3.3 Flash Duration and Flash Rate

Each convective cell had an average total flash (i.e. LDAR detected flashes only) duration (or total flash time interval) of 31.6 minutes. This duration was defined as the total time from when the first VHF source was detected to when the last IC flash occurred in a thunderstorm. The CG duration was defined in a similar way (i.e. time difference between first and last occurring CG) and was slightly lower at an average and median value of 25 minutes. It is important to note that case 34 had only one occurring CG, thus its CG flash duration and flash rate is represented as zero.

Williams (2001) describe total flash rates of typical non-severe, ordinary thunderstorms to be on the order of 3 flashes min^{-1}. On average, ordinary thunderstorms have low flash rates. Other studies in the last ten years using the LDAR network in Florida have confirmed the low total flash rates found in this storm type (e.g., Rison et al. 1996; Stanley et al. 1996). This current study had total flash rates that were half the

value found in Williams' study. Average and median flash rates (both total and CG) were calculated for the 37 cases by counting the number of flashes that occurred within each event and dividing by the thunderstorm total flash duration. The mean and median total flash rate as detected by LDAR was 1.4 and 1.3 flashes min^{-1}, respectively (Fig. 14). The average CG flash rate at 0.66 flashes min^{-1} for the 37 cases was lower than the mean total flash rate. Case 31 exhibited both the highest total flash rate and the greatest CG flash rate with 4.2 and 1.6 flashes min^{-1}, respectively. Just over 22% of the cases (i.e. cases 1, 8, 9, 10, 19, 20, 22, and 30) went against the trend of thunderstorms having greater IC flash rates than CG flash rates and recorded higher CG flash rates than IC flash rates. However, cases 8, 9, 10, and 29 actually recorded a greater number of CG flashes than flashes detected by LDAR alone. This trait goes against most lightning observations as it is generally accepted that cloud flashes usually outnumber ground flashes (MacGorman and Rust 1998, p. 190).

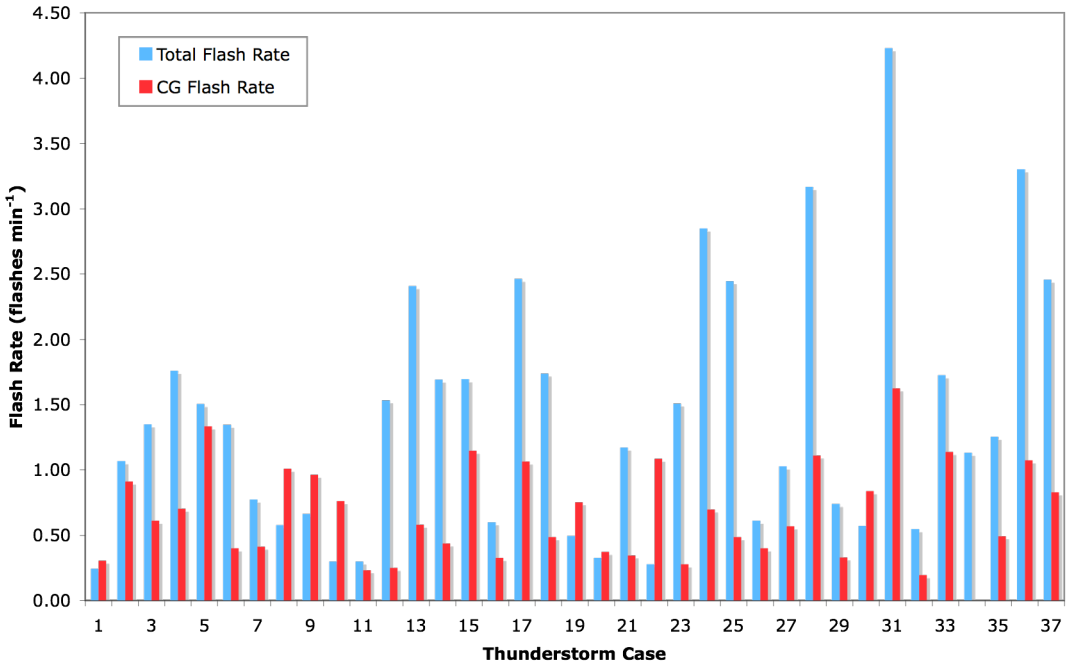

Fig. 14. Total flash rate (flashes min^{-1}) (blue bars) and CG flash rate (red bars) for each thunderstorm case. Note the variability between each case. Cases 1, 8, 9, 10, 19, 20, 22, and 30 recorded a greater CG flash rate than IC flash rate.

3.4 Percent Positive Flash

MacGorman and Rust (1998, p. 192) state that most ground flashes in isolated storms lower negative charge to ground. Flash statistics from a study by Orville (1994) show that less than 10% of all ground flashes in the United States lowered positive charge to the ground. In a later study by Orville et al. (2002), the occurrence of positive flashes was also below 10%, or 8.9% (when ignoring peak currents less than 10 kA) across the United States. The results of this study were about half of Orville's, with a

mean percent positive flash observance of 4.1% (Table 3). Moderate variability existed between each convective case, ranging from 0% to 23.1% positive flash occurrence. The standard deviation for each case was 5.8%. From Table 3, one can see that 21 of the 37 cases (~57%) contained no flashes lowering positive charge to ground.

However, there is strong seasonal variation in the positive ground flash percentage (MacGorman and Rust 1998, p. 192). All 37 cases in this study occurred during the warm season over Houston, and research has found that the positive flash percentage increases during cool seasons and peaks during the winter (e.g., Takeuti et al. 1977, 1978, Orville et al. 1987, Reap 1991).

As mentioned in Section 2.2, positive flashes with peak current of 10 – 20 kA were counted as CG only. However, according to Cummins et al. (2006), flashes in this range are likely a mix of IC and CG flashes. In this current study, 76% of all the positive CG flashes had peak currents between 10 - 20 kA. The greatest magnitude of positive peak current was 31.69 kA found in case 26.

3.5 Final Flash Observed

Also found was the occurrence and time delay of the final flash observed by either the NLDN or LDAR network (i.e. determining the type of flash that occurs last). In twenty-six of the thirty-seven cases (~70%), the last flash recorded was intracloud. The average time lag between the last CG and the last IC in these 26 events was 6.3 minutes. In seven of the remaining eleven cases that recorded a CG as the last flash, the

Table 3. Percent positive flash observance (PERCENT POSITIVE FLASH) as seen in each of the 37 cases. Average percent positive value listed at bottom of table.

CASE #	PERCENT POSITIVE FLASH
1	0.0
2	10.5
3	11.1
4	0.0
5	3.3
6	0.0
7	0.0
8	0.0
9	4.0
10	0.0
11	14.3
12	0.0
13	0.0
14	0.0
15	8.3
16	4.2
17	9.1
18	11.8
19	0.0
20	0.0
21	0.0
22	0.0
23	14.3
24	9.1
25	0.0
26	23.1
27	13.3
28	0.0
29	0.0
30	2.8
31	0.0
32	0.0
33	0.0
34	0.0
35	6.3
36	0.0
37	6.7
AVERAGE	**4.1%**

last intracloud flash led to the final CG discharge. Cases 3, 10, 26, and 29 experienced the final CG discharge on an average of 9.3 minutes after the last IC flash! In each of these events, there was no LDAR support (i.e. intracloud components) that accompanied these cloud-to-ground flashes. This time separation signature appears to be of no value to a forecaster because of the impossibility to know which IC flash will lead to the last CG flash.

4. DISCUSSION

Several studies have attempted to use total lightning (e.g. LDAR detected events) and CG flash data characteristics as precursors to differing meteorological phenomenon. Williams et al. (1989) state that the detection of total lightning in thunderstorms forming in weakly sheared environments (i.e. ordinary convection) provides one short-term warning for microburst hazards at low levels. Goodman et al. (1988) show that the peak flash rate occurred 4 minutes prior to the microburst onset in a storm in Alabama. Comparisons between ground lightning flash activity and rainfall have also been attempted. Holle and Bennett (1997) suggest that by using criteria based on the duration of ground flash activity, many flash floods in Arizona can be detected. Piepgrass et al. (1982) found that peak rainfall occurred within 10 minutes of peak flash rates in isolated storms over Florida.

4.1 Warning Time to First CG with LDAR Network

The effort to find a correlation between some specific threshold (whether with radar or total lightning networks) and the onset of CG lightning has been reviewed (see Sec. 1.5). Furthermore, a study by Goodman et al. (1988) showed that the first CG flash in microburst thunderstorm was preceded by the initial IC discharge by 5 minutes. In a sample of 13 storms over Houston, Motley (2006) found an average of 12 minutes between the first LDAR detected intracloud flash and the first CG discharge. Similar to

this study, Motley had significant variability among the studied cases. Even though the approach in his study and this current study was similar, the significant increase in the number of cases analyzed in this study possibly resulted in a shorter CG warning time. This difference is attributed to the limited total lightning data available at the time of his study.

Various warning time results of 37 isolated, ordinary thunderstorms over Houston have been presented. The average warning time for the first CG flash using the LDAR network alone was just over 3 minutes. This outcome was accomplished by comparing the time of first detected VHF source and the first NLDN detected cloud-to-ground flash. Originally, the idea that the real-time detection of total lightning by the LDAR network in Houston could serve as a practical tool in forewarning the public of cloud-to-ground lightning dangers that typically occur in this storm type. However, with 3 storms exhibiting a negative CG lead time (i.e. the first CG occurred before the first IC) and another 4 events possessing a zero CG lead time, hope that this would be a reliable tool has been removed. It is important to note that the aforementioned cases that revealed a negative CG warning time occurred during the first two LDAR operational lightning events. While the necessary number of sensors were operational during these two days (see Sec. 2.1), it is possible that detection errors of the newly functioning network could have resulted in "missed" VHF sources.

Another issue with using the LDAR network to forewarn the onset of CG activity is that three minutes may not be enough time for the network to process the first flashes of a newly developing thunderstorm and display them online. The following description

of the real-time aspects of LDAR is from personal communication with Joe Jurecka. Typically, the real-time detection of VHF sources by the LDAR network is mapped and viewed online (available from the World Wide Web at http://www.met.tamu.edu/ciams/ldar). However, in general, it takes between 30-75 seconds for the LDAR computer to create the positions of VHF sources and flashes the network detects in real-time. Once every two minutes, the main LDAR computer generates a new set of images to make available online. The web page is automatically refreshed by the client every 60 seconds. Therefore, it may take anywhere between 30 seconds and 4.5 minutes for new flash data to become available for use to forecasters, depending on when new data is available and when the website refreshes.

One can see that the processing time of the LDAR network over Houston can exceed the three minute CG warning time determined in this study. It appears that using the LDAR network alone in the real-time detection of IC flashes to forewarn CG onset is futile.

4.2 Warning Time to First CG with Radar

In this study, using the criteria of when the 30-dBZ contour first reaches the environmental -10°C isotherm proved to be the best method in forewarning the first CG lightning flash. This method had an average warning time of 16.1 minutes which is five times greater than the previously mentioned method. Using the threshold of 40-dBZ at -10°C demonstrated a better lead time than LDAR alone at 12.1 minutes (Table 2). The previous studies mentioned in Section 1.5 had similar CG lead times as compared to this

study. Gremillion and Orville (1999) found a median warning time of 7.5 min. when using the criteria of 40-dBZ at the -10°C temperature height for two consecutive volume scans. Hondl and Eilts (1994) found a 15 minute warning time between the first 10-dBZ echo aloft and the first detected CG lightning strike in Florida thunderstorms. The best predictor of CG onset in a study by Vincent et al. (2004) was the initiation of 40-dBZ at -10°C for one volume scan. This criterion brought about an average CG lead time of 14.7 minutes. Wolf (2006) used a slightly different approach than these other studies and found that a 40-dBZ height at least 2.4 km above the U-10L (the -10°C level within the thunderstorm updraft rather than the ambient environment) would be useful for predicting the cells that would go on and produce "frequent/numerous" lightning strikes to ground. In his study, no quantitative time was given for the separation between the radar characteristic and CG activity.

Several schools of thought exist in determining the best method to predict the onset of CG flashes using radar. One such disparity is how to define the time difference between the particular radar threshold and the first CG flash. In general, every radar volume scan's time stamp is labeled with the time value of the lowest (i.e. first) elevation scan in the volume. Some researchers then adjust their CG warning times due to the fact that radar scans upper-levels of a thunderstorm (i.e. -10°C level) a few minutes after the start of the volume scan (e.g. Vincent et al. 2004). Therefore, some believe that using the time at the beginning of the radar volume scan is not a true representation of the CG onset signature. In contrast, this present study calculated its warning time using the beginning of the radar volume scan in which 30-dBZ (or 40-

dBZ) first reached the -10°C level. We picked this method due to a forecaster's inability to "dissect" a radar volume scan. In real-time, a forecaster must wait for an entire radar volume scan to finish before being able to view it scan-by-scan. As soon as a volume scan is available to use and analyze, the radar is already on the next volume scan. The single elevation scans of this subsequent volume scan cannot be viewed until the entire volume is completed. At the NWS Weather Forecast Office (WFO) in Houston, forecasters can see each elevation scan in real-time and do not necessarily have to wait on the entire volume scan to finish. However, they are limited in what can be done with these individual real-time scans and typically just wait for the entire volume scan to finish before doing analyses (Joe Jurecka, personal communication).

Another question is whether the ambient environmental isotherm levels or the modified updraft isotherm levels should be used when doing radar based CG warning time studies. As mentioned in the first paragraph of this section, Wolf (2006) employs the use of the -10°C level within the thunderstorm updraft, which he labels U-10L. The purpose of this level is to bypass the impact of environmental entrainment on the updraft of the thunderstorm. Finding the U-10L in his study was achieved with actual and model-forecast soundings that were modified using surface observation data. Conversely, we used the environmental isotherm level in this current study because of the difficulty to quantitatively know the modified updraft temperature profile of a thunderstorm.

Utilizing a specific radar characteristic that precedes the onset of CG lightning activity proved to be a superior method than using the LDAR network alone. In addition,

the WSR-88D network is extensive compared to that of total lightning networks. Therefore, the forewarning of CG lightning using radar defined characteristics can be developed and employed in additional locations across the country.

4.3 Warning Time to Final CG

Several attempts were made to discover a feature derived from specific storm properties that could precede the last CG in isolated, ordinary thunderstorms. Previous studies have shown various observations that preceded the cessation of lightning activity in their samples. Christian et al. (1980) found that lightning activity ended when the radar echo reached its maximum height. Wolf (2006) described that the criteria used in his study to classify storms with no CG activity could be using for anticipating lightning cessation in electrified storms. He observed that when the 40-dBZ echo was observed at 8 kft below the -10°C level, there was a 100% probability of no cloud-to-ground lightning. When the 40-dBZ echo was observed between 5-7 kft below the -10°C height, there was a 94% probability of no CGs. Therefore, he suggests that either one of these criterion could be used in electrified storms to predict the end of lightning activity. This technique was not applied in his study but further work could test the plausibility of such relationship.

Finding such feature would be beneficial to forecasters that serve emergency managers in charge of escorting the public to safety when a CG lightning event occurs. Knowing when the final CG of any event has occurred would be valuable information for any community that is involved in outdoor sporting events, recreation, etc. In this current study, efforts were made to find a similar radar characteristic for forecasting the

onset of the first CG flash as described in Section 2.4.3 that can be applied to forecasting the last occurring CG flash. The best approach was found by averaging the radar characteristics (i.e. the maximum radar reflectivity value) at the -10°C height found in the volume scans prior to, during, and after the last CG flash. On average, the maximum radar reflectivity at -10°C for the volume scan prior to the last CG volume scan was 47 dBZ. The mean radar reflectivity was 43.7 dBZ during the last CG radar scan and 41.7 dBZ during the subsequent radar volume scan. Based on the average (median) of 37 ordinary thunderstorms over Houston, one can infer that the final CG flash will occur when the radar reflectivity value of 45-dBZ (40-dBZ) falls below the -10°C isotherm. As described in Section 3.2, using this method but at the freezing level yielded results that based on the average were acceptable, but the specific radar characteristic (i.e. 50-dBZ at 0°C) was not observed in every thunderstorm event presented in this study.

Variability did exist between each thunderstorm case when applying this previously mentioned method. Weak thunderstorms (i.e. 12 of 37 cases) had a tendency to experience the above pattern prior to CG cessation and strong thunderstorms (i.e. 6 of 37 cases) observed the 45-dBZ contour's descent below the -10°C level after the final CG flash.

5. CONCLUSION

Thirty-seven isolated, ordinary thunderstorms were examined over Houston, Texas. Storm events occurred in August and September 2005 and June and August 2006. Each cell was objectively picked using a set list of criteria and carefully examined using the WDSS-II GUI and several IDL programs. This storm type was picked due to the inability to forecast its occurrence of lightning coming to ground. Other storm types pose the same difficulty in forecasting CG flashes. However, the other common storm type to affect Houston is in the form of a squall line. Squall lines that typically affect Houston have already formed prior to entering LDAR range and proceed through the entire network, sometimes without much dissipation. Therefore, CG lightning has most likely initiated outside of Houston and its occurrence can be tracked with real-time displays of NLDN data. The need to forecast said CG lightning in Houston is quite low in most cases.

Analyses showed that using the LDAR network and the NLDN in conjunction with each other provided a mean CG warning time of only 3 minutes. This lead time was much lower than originally anticipated and when compared to the radar results in Section 3.2, did not provide much advancement in the CG forecasting realm. Using the criteria of when the 30-dBZ contour first reached the environmental -10°C isotherm proved to be the best method in forewarning the first CG lightning flash. The average CG warning time for this method was 16.1 minutes and was found to be similar to previous studies.

Similarly, the LDAR network did not prove to be a valuable tool in discerning when the last CG flash would occur based on the observed IC flash characteristics. In fact, it was found that in 70% of the cases, the last occurring flash was intracloud. Therefore, we attempted to find a radar characteristic that could forewarn the occurrence of the last CG flash in this storm type. Based on the average radar characteristics during the last CG flash in each thunderstorm case, CG activity comes to an end when the 45-dBZ echo falls below the -10°C isotherm. However, more work needs to be done on a larger sample and perhaps a different geographic location to see if this pattern holds true.

Flash rate characteristics resembled those of previous studies (i.e. low flash rates in accordance to storm type) (e.g., Rison et al. 1996; Stanley et al. 1996). The average total flash rate was on the order of 1.4 flashes min^{-1} and the average CG flash rate was 0.7 flashes min^{-1}. A 4.1% positive flash occurrence, according to this study, is comparable to other studies (e.g., Orville 1994; Orville et al. 2002). Steiger et al. (2002) shows that 5% of the ground flashes recorded over Houston were positive, with an increase to 17% during the winter months. It is important to note that in all the statistics gathered and calculated, variability among each case was quite high.

VHF sources are optimally detected within a 100 km range from the LDAR center (Ely et al. 2007) while the NLDN has a detection efficiency of 90-95% within the interior of the United States (Cummins et al. 2006). Detection efficiencies that remain slightly less than perfect for each network may have allowed for some error when analyzing VHF sources and ground flashes for each convective case. Cases 1, 8, 9, 10, 19, 20, 22, and 30 exhibited this possible error. Contrary to common lightning

characteristics, these eight cases showed a higher CG flash rate than total flash rate. In addition, cases 8, 9, 10, and 29 actually recorded a greater number of CG flashes than IC flashes, which is contrary to typical lightning characteristics (MacGorman and Rust 1998, p. 190). These discrepancies raise concern for the detection efficiency of either network on these days.

This study was limited to 17 months (i.e. August 2005 – December 2006) of LDAR data, therefore, future studies hope to increase the number of thunderstorm cases to analyze as the LDAR network continues to observe more lightning events. A similar study in differing geographic regions of the country would be beneficial as to observe if these lightning characteristics vary depending on latitude, longitude, or climate. One target location could be the Dallas – Ft. Worth (DFW) area that has a preexisting LDAR network in operation. Motley (2006) found a 6 minute time separation between the first VHF source and the first CG in a small sample of 9 storms over DFW. Future work for the Houston area needs to utilize a large sample of both electrified and non-electrified storms so that comparisons between the radar reflectivity results found in this study can be compared to non-electrified storms (e.g. Gremillion and Orville 1999, Vincent et al. 2004).

REFERENCES

Berger, K., 1978: Blitzstrom-Parameter von Aufwartsblitzen. *Bull. Schweiz. Elektrotech. Ver.*, **69**, 353-360.

Brown, R.A., V.T. Wood, and D. Sirmans, 2000: Improved WSR-88D scanning strategies for convective storms, *Wea. Forecasting*, **15**, 208-220.

Buechler, D. E., and S. J. Goodman, 1990: Echo size and asymmetry: Impact on NEXRAD storm identification. *J. Appl. Meteor.* **29**, 962-969.

Byers, H. R., and R. R. Braham, Jr., 1949: *The Thunderstorm*. Supt. of Documents, U. S. Government Printing Office, Washington DC, 287 pp.

Christian, H.J., C.R. Holmes, J.W. Bullock, W. Gaskell, A.J. Illingworth, and J. Latham, 1980: Airborne and ground-based studies of thunderstorms in the vicinity of Langmuir Laboratory. *Q. J. Roy. Meteor. Soc.*, **106**, 159-174.

Cummins, K. L., J. A. Cramer, C. Biagi, E. P. Krider, J. Jerauld, M. A. Uman, and V.A. Rakov, 2006: The U.S. National Lightning Detection Network: Post-upgrade status. *2nd Conf. on Meteorological Applications of Lightning Data*, Amer. Meteorol. Soc., Atlanta, paper 6.1

Curran, E. B., R. L. Holle, R. E. Lopez, 2000: Lightning casualties and damages in the United States from 1959 to 1994. *J. Climate*, **13**, 3448–3464.

Dye, J. E., W. P. Winn, J. J. Jones, and D. W. Breed, 1989: The electrification of New Mexico thunderstorms. 1. The Relationship between precipitation development and the onset of electrification. *J. Geophys. Res.*, **94**, 8643-8656.

Ely, B. L., R. E. Orville, L. D. Carey, and C. L. Hodapp, 2007: Evolution of the total lightning structure in a leading-line, trailing-stratiform mesoscale convective system over Houston, Texas. *J. Geophys. Res.*, In Press.

Goodman, S.J., D.E. Buechler, P.D. Wright and W.D. Rust, 1988: Lightning and precipitation history of a microburst-producing storm. *Geophys. Res. Lett.,* **15**, 1185-1188.

Gremillion, M., and R. E. Orville, 1999: Thunderstorm characteristics of cloud-to-ground lightning at the Kennedy Space Center, Florida: A study of lightning initiation signatures as indicated by the WSR-88D radar, *Wea. Forecasting*, **14**, 640-649.

Hondl, K. D., and M. D. Eilts, 1994: Doppler radar signatures of developing thunderstorms and their potential to indicate the onset of cloud-to-ground lightning. *Mon. Wea. Rev.*, **122**, 1818-1836.

Huff, F.A., and S.A. Changnon, Jr., 1973: Precipitation modification by major urban areas, *Bull. Amer. Meteor. Soc.*, **54**, 1220-1232.

Imyanitov, I. M., Y. V. Chubarina, and Y. M. Shvarts, 1971: Electricity of clouds. 92 pp., Leningrad: Gidrometeoizdat (NASA Technical Translation from Russian NASA, TT-F-718, 1972).

Johnson, J. T., P. L. MacKeen, A. Witt, E. D. Mitchell, G. J. Stumpf, M. D. Eilts, and K. W. Thomas, 1998: The storm cell identification and tracking algorithm: An enhanced WSR-88D algorithm. *Wea. Forecasting*, **263**, 263-276.

Kitagawa, N., M. Brook, and E. J. Workman, 1962: Continuing currents in cloud-to-ground lightning discharges. *J. Geophys. Res.*, **67**, 637 – 647.

Krehbiel, P. R., 1986: The electrical structure of thunderstorms. *The Earth's Electrical Environment*, National Academic Press, 90-113.

Krider, E. P., R. C. Noggle, A. E. Pifer, and D. L. Vance, 1980: Lightning direction-finding systems for forest fire detection. *Bull. Amer. Meteor. Soc.*, **61**, 980-986.

Lakshmanan, V., T. Smith, G. Stumpf, and K. Hondl, 2007: The warning decision support system – integrated information. *Wea. Forecasting*, **22**, 596-612.

Lennon, C., and L. Maier, 1991: Lightning mapping system, *NASA Conf. Publ.*, **3106**(2), 89.1-89.10.

Lhermitte, R. M., and P. Krehbiel, 1979: Doppler radar and radio observations of thunderstorms. *IEEE Trans. Geosci. Electron.,* **17,** 162–171.

Livingston, J.M., and E. P. Krider, 1978: Electric fields produced by Florida thunderstorms, *J. Geophys. Res.*, **83**, 385-401.

MacGorman, D. R., and W. D. Rust, 1998: *The Electrical Nature of Storms*. Oxford University Press, 442 pp.

Michimoto, K., 1991: A study of radar echoes and their relation to lightning discharge of thunderclouds in the Hokuriku district. Part I: Observations and analysis of thunderclouds in summer and winter. *J. Meteor. Soc. Japan*, **69**, 327-335.

Moore, C. B., and B. Vonnegut, 1977: The thundercloud. *Lightning, Vol. 1: Physics of Lightning*. R. H. Golde, Ed., Academic Press, 64-98.

Motley, S.M., 2006: *Total Lightning Characteristics of Ordinary Convection*, M.S. Thesis, Texas A&M University.

Orville, R. E., 1991: Lightning ground flash density in the Contiguous United States – 1989. *Mon. Wea. Rev.*, **119**, 573-577.

--------, 1994: Cloud-to-ground lightning flash characteristics in the contiguous United States: 1989-1991, *J. Geophys. Res.*, **99**, 10833-10841.

--------, and G. R. Huffines, 2001: Cloud-to-ground lightning in the USA: NLDN results in the first decade 1989-1998, *Mon. Wea. Rev.*, **129**, 1179-1193.

--------, R. W. Henderson and L. F. Bosart, 1983: An East Coast lightning detection network, *Bull. Amer. Met. Soc.*, **64**, 1029-1037.

--------, R. A. Wiesman, R. B. Pyle, R. W. Henderson, and R. E. Orville, Jr., 1987: Cloud-to-ground lightning characteristics from June 1984 through May 1985. *J. Geophys. Res.*, **92**, 5640-5644.

--------, G. R Huffines, W. R. Burrows, R. L. Holle, and K. L. Cummins, 2002: The North American Lightning Detection Network (NALDN) – First results: 1998-2000. *Mon. Wea. Rev.*, **130**, 2098 – 2109.

Piepgrass, M.V., E.P. Krider, and C.B. Moore, 1982: Lightning and surface rainfall during Florida thunderstorms. *J. Geophys. Res.*, **87**, 193-201.

Rakov, V.A., and M. A. Uman, 2003: *Lightning: Physics and Effects*. Cambridge University Press, 687 pp.

Reap, R. M., 1991: Climatological characteristics and objective prediction of thunderstorms over Alaska. *Wea. Forecasting*, **6**, 309-319.

Rison, W. P., P. Krehbiel, L. Maier, and C. Lennon, 1996: Comparison of lightning and radar observations on a small storm at Kennedy Space Center, Florida. Preprints, *Tenth Int. Conf. on Atmospheric Electricity*, Osaka, Japan, Amer. Meteor Soc., 196-199.

Simpson, Sir G., and F. J. Scrase, 1937: The distribution of electricity in thunderclouds, *Proc. Roy. Soc. Lond., A,* **161**, 309-352.

--------, and G. D. Robinson, 1941: The distribution of electricity in thunderclouds, II, *Proc. Roy. Soc. Lond., A,* **177**, 281-328.

Simpson, J.E., 1994: *Sea Breeze and Local Wind*. Cambridge University Press, 234 pp.

Smith, J.R., H.E. Fuelberg, and A.I. Watson, 2005: Warm season lightning distributions over the Northern Gulf of Mexico Coast and their relation to synoptic-scale and mesoscale environments, *Wea. Forecasting*, **20**, 415-438

Stanley, M., P. Krehbiel, L. Maier, and C. Lennon, 1996: Comparison of lightning observations from the KSC LDAR system with NEXRAD radar observations, Preprints, *Tenth Int. Conf. on Atmospheric Electricity*, Osaka, Japan, Amer. Meteor. Soc., 224-227.

Steiger, S. M., R. E. Orville, and G. Huffines, 2002: Cloud-to-ground lightning characteristics over Houston, Texas: 1989-2000. *J. Geophys. Res.*, **107**, D11, 10.1029/2001JD001142.

Takahashi, T., 1978: Riming electrification as a charge generation mechanism in thunderstorms. *J. Atmo. Sci.*, **35**, 1536-1548.

Takeuti, T., M. Nakano, H. Ishikawa, and S. Israelsson, 1977: On the two types of thunderstorms deduced from cloud-to-ground discharges oversized in Sweden and Japan. *J. Meteor. Soc. Japan*, **55**, 613-616.

--------, --------, M. Brook, D. J. Raymond, and P. Krehbiel, 1978: The anomalous winter thunderstorms of Hokuriku coast. *J. Geophys. Res.*, **83**, 2385-2394.

Uman, M. A., 1968: *Lightning*. McGraw-Hill Press, 254 pp.

--------, 1971: *Understanding Lightning*. Bek Technical Publications, 166 pp.

--------, 1987: *The Lightning Discharge*. International Geophysics series; v. 39, Academic Press, xii, 377 pp.

Vincent, B. R., L. D. Carey, D. Schneider, K. Keeter, and R. Gonski, 2004: Using WSR-88D reflectivity for the prediction of cloud-to-ground lightning: A Central North Carolina study. *Natl. Wea. Dig.*, **27**, 35-44.

Wacker, R. S. and R. E. Orville, 1999: Changes in measured lightning flash count and return stroke peak current after the 1994 U. S. National Lightning Detection Network upgrade; Part II: Theory, *J. Geophys. Res.*, **104**, 2159-2162.

Weisman, M. L., and J. B. Klemp, 1982: The dependence of numerically simulated convective storms on vertical wind shear and buoyancy. *Mon. Wea. Rev.*, **110**, 504-520.

--------, and --------, 1984: Characteristics of isolated convective storms. *Mesoscale Meteorology and Forecasting*. P. S. Ray, Ed. Amer. Meteor. Soc., 331-358.

--------, and --------, 1986: The structure and classification of numerically simulated convective storms in directionally varying wind shears. *Mon. Wea. Rev.*, **112**, 2479-2498.

Williams, E. R., 2001: The electrification of severe storms. *Severe Convective Storms*. C. A. Doswell, Ed. Amer. Meteor. Soc., 527-561.

--------, M. E. Weber, and R. E. Orville, 1989: The relationship between lightning type and convective state of thunderclouds. *J. Geophys. Res.*, **94**, 13213-13220.

Wilson, C. T. R., 1916: On some determinations of the sign magnitude of electric discharges in lightning flashes. *Proc. Roy. Soc. Lond.*, **92**, 555-574.

--------, 1920: Investigations on lightning discharges and on the electric field of thunderstorms. *Phil. Trans. Roy. Soc. Lond.*, **221**, 73-115.

--------, 1929: Some thundercloud problems. *J. Franklin Inst.*, **208**, 1-12.

Wolf, P., 2006: Anticipating the initiation, cessation, and frequency of cloud-to-ground lightning, utilizing WSR-88D reflectivity data. *NWA Electronic Journal of Operational Meteorology*, December 2006.

VITA

Nathan Chase Clements was born to Mr. and Mrs. Wendel Keith Clements of Canyon, TX. He graduated from Canyon High School in May of 2001.

In May of 2005, Nathan Clements graduated Cum Laude from Texas A&M University with a B.S. degree in Meteorology. He received his M.S. degree in Atmospheric Sciences from Texas A&M in December 2007. His current address is:

17200 Bobbye Ln.

Canyon, TX 79015